# SEISMIC IMAGING TO CONSTRAIN GROUNDWATER MODELS FOR A BETTER UNDERSTANDING AND MANAGEMENT OF WATER QUALITY IN COASTAL BENIN, WEST AFRICA: A SALTWATER INTRUSION PROBLEM

by

Kyle Michael Lindsay

A thesis

submitted in partial fulfillment

of the requirements for the degree of

Master of Science in Geophysics

Boise State University

May 2015

BOISE STATE UNIVERSITY GRADUATE COLLEGE

**DEFENSE COMMITTEE AND FINAL READING APPROVALS**

of the thesis submitted by

Kyle Michael Lindsay

Thesis Title: Seismic imaging to constrain groundwater models for a better understanding and management of water quality in coastal Benin, West Africa: A saltwater intrusion problem

Date of Final Oral Examination: 12 December 2014

The following individuals read and discussed the thesis submitted by student Kyle Michael Lindsay, and they evaluated his presentation and response to questions during the final oral examination. They found that the student passed the final oral examination.

| | |
|---|---|
| John H. Bradford, Ph.D. | Chair, Supervisory Committee |
| Lee M. Liberty | Member, Supervisory Committee |
| James P. McNamara, Ph.D. | Member, Supervisory Committee |

The final reading approval of the thesis was granted by John H. Bradford, Ph.D., Chair of the Supervisory Committee. The thesis was approved for the Graduate College by John R. Pelton, Ph.D., Dean of the Graduate College.

# ACKNOWLEDGMENTS

I express my profound gratitude to my advisor, Dr. John Bradford, for his invaluable teaching and guidance during my career at Boise State University. I have had the pleasure of learning, working, and traveling with Dr. Bradford and feel truly lucky to have had such an exceptional mentor and travel buddy. I also sincerely thank Dr. Stephen Silliman, Dr. Nicaise Yalo, and Dr. Moussa Boukari for all of their support on this project. This work would not have been possible without their help and expertise.

I thank Geoscientists Without Borders for providing funding for this project and making this work possible. I also thank the Society of Exploration Geophysicists for a travel grant that provided funding to a conference to present this work, and Boise State University for a research grant that helped fund field work for this project. I also thank Micron Engineering and Mala Geoscience for donating equipment to the project, and Delta Airlines for allowing us to ship our equipment free of charge.

I thank my committee members Lee Liberty and Dr. James McNamara for their interest in this work as well as their time and suggestions. I especially thank Lee Liberty for all of his guidance over the last six years as well as the many opportunities he has given me for work and research.

I thank Dr. Esther Babcock, Dr. Thomas Blum, and Dr. Dylan Mikesell for being a huge part of this project and for their invaluable help with data collection, presentation preparation, and thoughtful discussions.

For this project I spent one month at the University of Lausanne, Switzerland,

working on extracting geostatistics from seismic reflection data we collected in Bénin. I thank Dr. James Irving for hosting me during this trip and sharing with me his knowledge of stochastic theory and geostatistics.

I thank all the students from the Université d'Abomey Calavi and l'Université Nice Sophia Antipolis. I especially thank Bénito Koukpohounsi and Romuald Kopessi for their help with data collection and for showing me an unforgettable time in Bénin. I also especially thank our driver and ambassador to Bénin, Yakoubou, for all of his help with logistics and data collection.

Last but not least, I thank all my friends and family, especially my parents Denise and Robert for all of their support, and Larry Otheim, Clinton Colwell, Erin Murray, and Mitchell Hopkins for making sure I had plenty of distractions from work.

# ABSTRACT

The coastal city of Cotonou in Bénin, West Africa, is a large population center that is facing a serious threat to the sustainability of its fresh water supply. Cotonou relies on groundwater derived from the Godomey aquifer for its domestic water supply. The aquifer is undergoing saltwater intrusion due to an increase in pumping to accommodate a growth in population. Hence, there is substantial interest in better characterizing the groundwater system for the purpose of determining appropriate management strategies to ensure sustainability of this freshwater resource.

I collected seismic reflection data along 15 transects to characterize the geometry of the Godomey aquifer system. I used standard high-resolution seismic methods to image the upper 200 meters using a sledgehammer source and a 120-channel recording system. Three transects were processed with an iterative updating flow that includes prestack depth migration, residual moveout analysis and reflection tomography, while the remaining 12 transects were processed with routine processing flows and poststack time migration. I identified one unconfined aquifer and three confined aquifers separated by reflective clay layers. Some transects showed areas of truncated reflectors which I interpret as channels that could provide potential high permeability conduits for saltwater flow to the Godomey well field.

I updated the aquifer geometry of the existing hydrologic model based on the seismic reflection data and used a three-dimensional finite difference groundwater model to evaluate the impact of the updated geometry on groundwater flow. The updated groundwater model predicts increased recharge from Lake Nokoué, a shallow

lake with elevated chloride concentrations that borders the eastern edge of the primary production well field.

# TABLE OF CONTENTS

# LIST OF TABLES

# LIST OF FIGURES

# CHAPTER 1

# INTRODUCTION

Coastal groundwater resources represent a critical component of available fresh water for rising population densities in coastal cities. Enhanced dependency on coastal groundwater has resulted in symptoms of over-extraction in many coastal regions around the world, namely excessive storage depletion and saltwater intrusion into fresh water aquifers (Bray *et al.*, 2007; Vandenbohede *et al.*, 2009; Werner, 2010; Silliman *et al.*, 2011). While saltwater intrusion is the primary concern for these coastal regions, many coastal aquifers are also susceptible to pollution by urban, industrial, and agricultural activities (Boukari *et al.*, 1996). Additionally, coastal aquifers are highly sensitive to the influences of climate change, which is expected to produce rising ocean levels and modified groundwater recharge. As a result of anthropogenic pressures, detailed characterization of groundwater quality and quantity in coastal regions has become necessary to properly manage these water supplies. While saltwater intrusion is a problem for coastal populations around the world, developing countries often lack the expertise and equipment to properly characterize and manage saltwater intrusion. As a result of these resource deficiencies, the problem of saltwater intrusion is likely to worsen in developing countries, where access to fresh water may already be limited. One such area that is experiencing these pressures is the coastal city of Cotonou in Bénin, West Africa.

According to the World Economic Forum (Schwab *et al.*, 2010), Bénin has become the most competitive economy in the West African Economic and Monetary Union due to a number of economic reforms enacted over the past decade. Despite these advances, Bénin remains economically underdeveloped with a significant dependence on subsistence agriculture (CIA, 2013). Bénin currently ranks 165 out of 187 countries on the United Nation's International Development Indicator that integrates information such as economic growth, income, education, and health (Khalid, 2014). This index also indicates that roughly 47% of the Bénin population lives below the poverty threshold.

Cotonou is Bénin's largest city with a population of 1.5 - 2.0 million people. The city lies in the southeast of the country along the Atlantic Ocean (Figure 1.1). Currently, the annual rate of urbanization in Bénin is approximately four percent. The growth of the urban population has necessitated an increase in the pumping rate from the city's primary well field, known as the Godomey well field. The well field lies approximately 5 km north of the Atlantic Ocean and is bordered on the east by Lake Nokoué, a large shallow lake with elevated chloride concentrations through the majority of the year. Increased pumping has been accompanied by an increase in salinity in the eastern portion of the well field, closest to Lake Nokoué.

The two potential sources of salinity in the well field are the Atlantic Ocean and Lake Nokoué. Several of the deeper aquifer units extend beneath the Atlantic Ocean, and therefore may be hydraulically connected to ocean waters. However, a previous study by Silliman *et al.* (2010) showed that wells closest to the ocean give no indication of increased salinity in the deeper aquifers. Conversely, all of the wells showing increased salinity are close to Lake Nokoué. Additionally, initial hydrologic models indicate that there is a groundwater divide between the Atlantic

Ocean and the Godomey well field and that Lake Nokoué is the likely source of salinity (Boukari *et al.*, 2008). These models predict that increased pumping will result in greater recharge being derived from the western part of Lake Nokoué, consistent with observations of increased salinity in wells closest to the lake (Silliman *et al.*, 2010).

While intrusion of saline waters from Lake Nokoué is the immediate threat to the Godomey aquifer, urbanization is resulting in increased development in the immediate vicinity of the Godomey well field, leading to greater risk of anthropogenic release of hazardous groundwater contaminants. Further complicating the system is the city of Ganvié, a city of approximately 30,000 people, built entirely on stilts in Lake Nokoué. The presence of this lake city and a large reliance on the lake for fishing has resulted in severe manipulation of the lake for waste disposal, navigation, and fish farming.

In light of the various factors endangering the drinking water supply of Cotonou, it is critical that good management decisions are made now to sustain a viable source of fresh water for this growing urban area. The management plan must actively minimize the encroachment of saline water from Lake Nokoué while at the same time mitigating the risk of hazardous anthropogenic contamination related to increased development. To achieve these management goals, an accurate groundwater model is needed to confidently predict groundwater flow and recharge behavior based on future water management scenarios (i.e. new well locations and pumping strategies).

While initial hydrologic models by Boukari *et al.* (2008) and Silliman *et al.* (2010) provide general information about the aquifer system, they are not yet at the stage of a quantitative management tool where data driven management decisions can be made. In particular, challenges remain in the modeling effort in terms of the temporal/spatial distribution of hydraulic head. The aquifer geometry of the current hydrologic model is based on analysis of well log data that is limited by the areal

extent of the wells in the Godomey well field. There have been no wells drilled in Lake Nokoué. Consequently, little is known about the geology underlying the lake and how it is connected to the geology in the well field.

One of the key characterization needs identified by Silliman *et al.* (2010) is mapping of the primary water bearing units to better understand and quantify the lateral continuity of flow paths. Quantifying the continuity of these units is necessary to improve the spatial resolution of the current hydrologic model and to determine transport pathways between the recharge areas in Lake Nokoué and the Godomey well field.

This research aims at using geophysical techniques to characterize the Godomey aquifer and address the need for a more refined hydrologic model.

## 1.1 Background

The Republic of Bénin (Figure 1.1) is located in Western Africa, and is bordered by Nigeria and Togo on the east and west respectively, with the southern coastline bordering the Atlantic Ocean. Bénin has a total land area of approximately 111,000 $km^2$, comprised mostly of flat plains in the south with some hills and low mountains in the north. The 2013 census estimated a population of 10.3 million, with an annual growth rate of 2.8%/yr (CIA, 2013).

The Document of National Policy of Water (Lafia, 2005) estimates the internal and external contributions to Bénin water resources to be approximately 25 billion $m^3$/yr. The same document notes that an increase in population would drastically reduce the quantity of water available per capita, assuming that these resources remain constant. In 1990 for example, the population was approximately 4.5 million people,

and the availability of water resources per capita was 5825 $m^3$/yr (Boukari *et al.*, 2008). Conservative estimates at the time of that study estimated the population of Bénin to be 11.3 million people by 2025, which reduces the quantity of water available per capita to 2293 $m^3$/yr. It is evident from the most recent census data that population growth has been far more rapid than even conservative estimates, with the new projected population estimate of almost 14 million people by 2025. This reduces the quantity of water available per capita to 1785 $m^3$/yr, placing Bénin in the category of countries with a grave shortage of water. These estimates assume that water availability in Bénin remains the same, and does not change as a result of climatic variability.

To accommodate this rapid population growth, more production wells have been added and pumping rates have increased. For example, eight additional wells were drilled during the period of 2001-2002, placing the total number of production wells at 24, each pumping 24 hours a day (Boukari *et al.*, 2008). The pumped discharge has continuously increased, from 5000 $m^3$/day in 1970 to 50,000 $m^3$/day in 2004 (Boukari *et al.*, 2008). The impact of intensive pumping on the groundwater is observed as a progressive decline of hydraulic heads in observation piezometers, and saltwater intrusion in select production wells (Boukari *et al.*, 1996) (Figure 1.2).

## 1.2 Survey Area

While saltwater intrusion has affected aquifers in all coastal regions of Bénin, this work focuses on south-central Bénin, near the population center of Cotonou. In particular, this study was undertaken near the the city's primary well field, known as the Godomey well field (Figure 1.1). Land use in the region varies from major urban

development around Cotonou to small rural villages (Silliman *et al.*, 2010). Economic growth has driven an increased need for infrastructure in the region. As a result, substantial portions of the land have been manipulated for construction, leading to decreased local recharge and increased runoff. Consequently, surface flooding during the rainy season has become a serious problem for urban Cotonou (Silliman *et al.*, 2010). Outside of the urban area, much of the land remains open wetlands. These wetlands are interspersed with small villages, where the population has infilled the wetlands in support of construction of homes and agricultural activities. Again, this manipulation of land has led to decreased recharge and increased runoff, causing flooding during the rainy season in many of these rural villages. This manipulated land use not only modifies the recharge of groundwater in these areas, but also increases the potential risk of anthropogenic pollution due to the standing flood waters in the city and rural villages.

## 1.3 Hydrogeological Setting

The Godomey well field lies on the south-eastern portion of the Plateau of Allada, in the coastal sedimentary basin of Bénin (Figure 1.3). The geology of the sedimentary basin has been previously described by multiples authors (Blivi *et al.*, 2002; Barthel *et al.*, 2008; Boukari *et al.*, 2008; Barthel *et al.*, 2009; Alassane *et al.*, 2009) and is comprised of three primary lithologic units consisting of a clayey-sand, sandy-clay, and sand of Pleistocene, Pliocene, and Miocene age respectively. These layers make up the coastal aquifer system and rest in angular unconformity on a highly heterogeneous clay/marl Eocene substratum between 180 - 220 m depth.

The geology in the production zone is comprised of interbedded sands, silts, and

clays that form four primary aquifers separated by confining clay layers (Figure 1.4). For clarity, I will refer to these aquifers as U1, C1, C2, and C3 where U1 is the top unconfined aquifer and C1, C2, and C3 are the three confined aquifers in order of increasing depth (Figure 1.4). Thicknesses range from 10 - 50 m for the sandy aquifer units and 5 - 10 m for the confining clay layers. The lithology dips slightly to the south, with several of the deeper aquifer units extending below the Atlantic Ocean, potentially exposing them to seawater influx directly from the ocean.

Recent hydrologic data has brought into question the validity of this simplified geologic model and suggests the confinement of aquifers in the region may not be complete (Figure 1.5). Figure 1.5 shows relative water levels in two piezometers screened at different depths and located approximately 1.3 km apart (PZ-PADER and PZ-SONEB; refer to Figure 2.3). The shallow aquifers (C1 and C2) and the deep aquifer (C3) are responding to variations in pumping pressure simultaneously, indicating the aquifers are hydraulically connected in this region.

## 1.4 Surface Hydrology

The study area near the Godomey well field lies approximately 5 km north of the Atlantic Ocean and is bordered on the east by Lake Nokoué, a large shallow lake (up to 3 m depth; Figure 1.3). Lake Nokoué is dynamic in terms of both hydraulics and water quality. Field data (water levels and measures of specific conductance in both the lake and groundwater) suggest active interaction of the lake with river inflows from the north, the ocean to the south (via an open channel connecting the lake to the ocean), and the groundwater system. Specifically, during periods of low precipitation, there is strong similarity in water level variations observed in the lake and in wells

within the region of the Godomey well field. These periods are accompanied by active exchange of lake and ocean via the channel connecting the lake to the ocean and increasing conductivity in the lake to a maximum (dependent on location in the lake) between 50% and 100% of the conductivity (salinity) of the ocean water (Silliman *et al.*, 2010). In contrast, periods of heavy precipitation are accompanied by increase in water level in the lake disproportionate with water level increase observed in the groundwater. Further, water inflow via the rivers during periods of precipitation results in flushing of salinity from the lake. Significantly, the southwestern region of the lake (the region closest to the well field) shows elevated conductance (salinity) even during periods in which the lake water is elevated following precipitation. This suggests this region of the lake as a possible region of recharge to the groundwater immediately east of the Godomey Well Field with water containing elevated salinity.

Lake Nokoué is fed from the Sô River in the northwest and the Djonou River in the southwest (Figure 1.3). During the rainy season, these rivers carry freshwater to Lake Nokoué. During the dry season, sea water from the Atlantic enters Lake Nokoué (Boukari *et al.*, 2008). This seasonal increase in Lake Nokoué saltwater causes reverse flow into the tributaries, making the portions of the Sô and Djonou Rivers near the lake brackish for the majority of the year.

## 1.5 Motivation

One of the key characterization needs for improving the current hydrologic model is to map the primary hydrostratigraphy to constrain the continuity of the flow pathways. Quantifying the continuity of these units is necessary to determine transport pathways between the recharge areas in Lake Nokoué and the Godomey well field. While

well borings, pump tests, and chemical sampling provide critical information about bulk aquifer properties, these measurements are limited in areal extent and do not adequately constrain the lateral continuity of aquifer units, which has a major impact on the aquifer response to pumping.

In the coastal plain environment, seismic reflection and electrical methods are well suited to imaging the primary geologic units (to establish continuity or lack thereof), identify regional variation in water levels, and constrain the spatial/temporal distribution of saltwater/freshwater interfaces. The two geophysical methods are sensitive to different physical properties and a number of authors have demonstrated that these measures provide complimentary information that can substantially improve the subsurface characterization (Bowling *et al.*, 2007; Chen *et al.*, 2006; Demanet *et al.*, 2001; Ferguson *et al.*, 1999; Šumanovac, 2006; Shtivelman and Goldman, 2000).

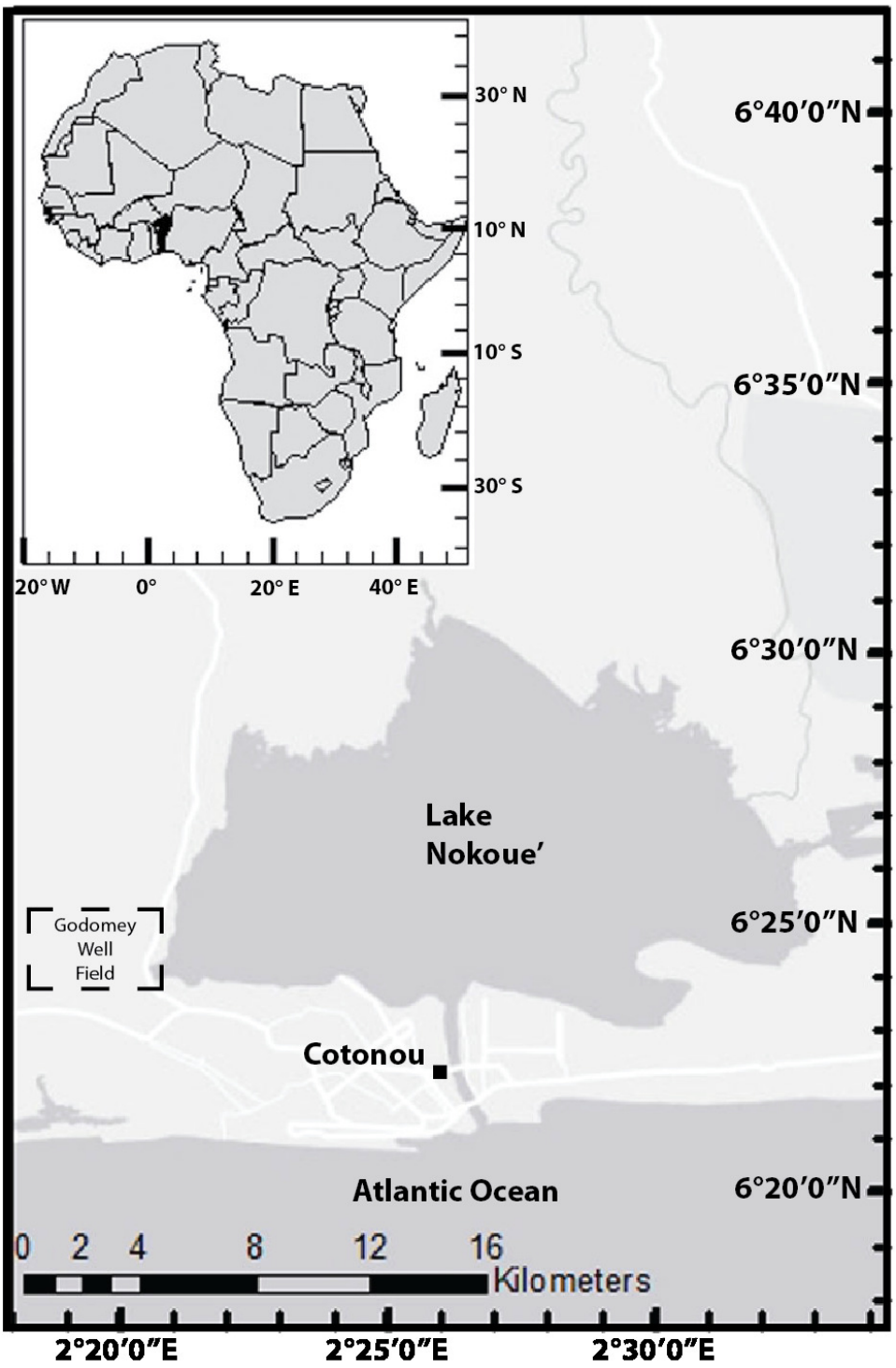


Figure 1.1: Inset map of Africa highlighting the location of Bénin, shown in black, and the regional map of coastal Bénin showing the city of Cotonou and Lake Nokoué. The Godomey well field is shown with the dashed box.

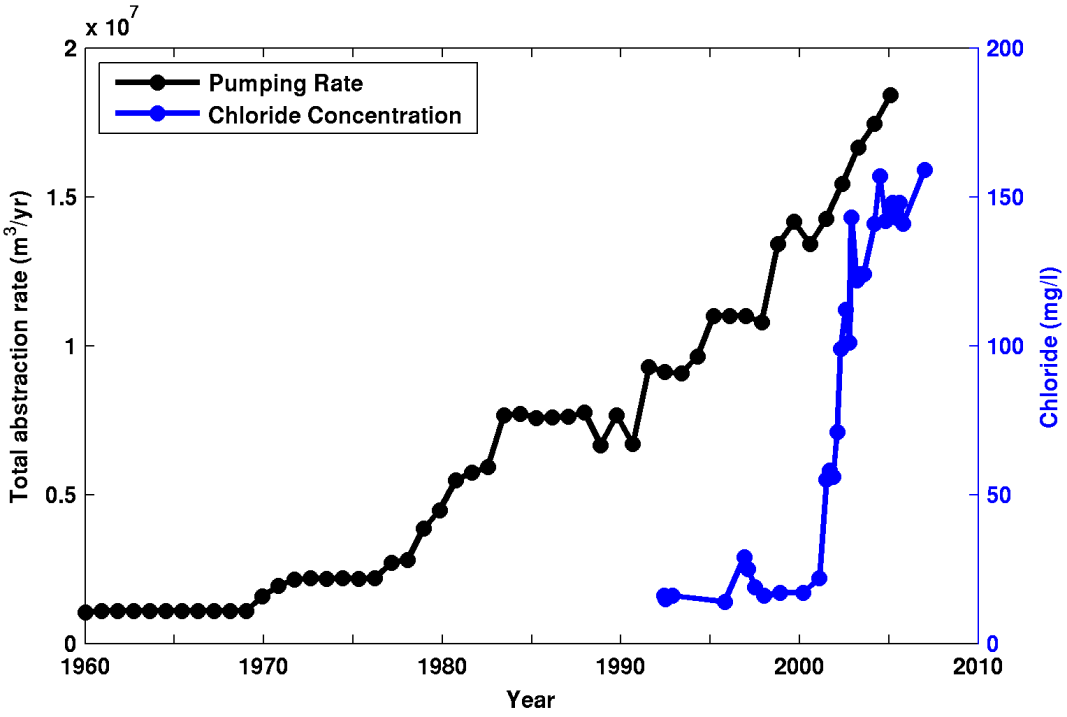


Figure 1.2: Evolution of the pumping rate in the Godomey well field (black) and chloride concentration in well F11 (blue). The pumping rate of the Godomey well field has increased on average by about 900,000 $m^3$/yr/yr since 1990, and has been accompanied by a rapid increase in chloride concentration beginning in the year 2000 (modified from Silliman *et al.*, 2010).

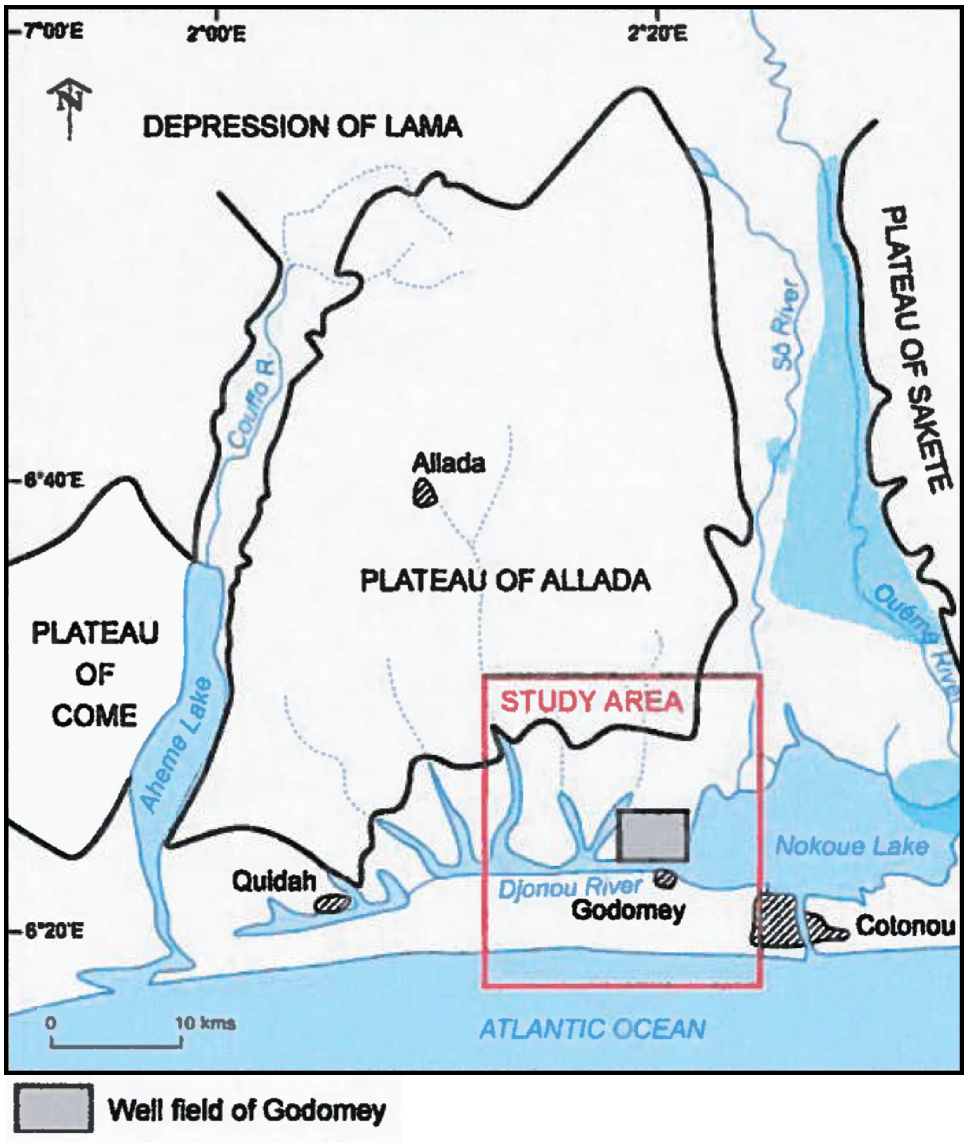


Figure 1.3: Map of lakes and rivers in the area of study (highlighted in red box). The Godomey well field (gray box) lies along the western shores of Lake Nokoué, with its southern edge bounded by the Djonou River. Lake Nokoué is connected to the Atlantic Ocean via a man-made canal. The western portion of Lake Nokoué is fed by the Djonou River which carries brackish water (modified from Boukari *et al.*, 2008).

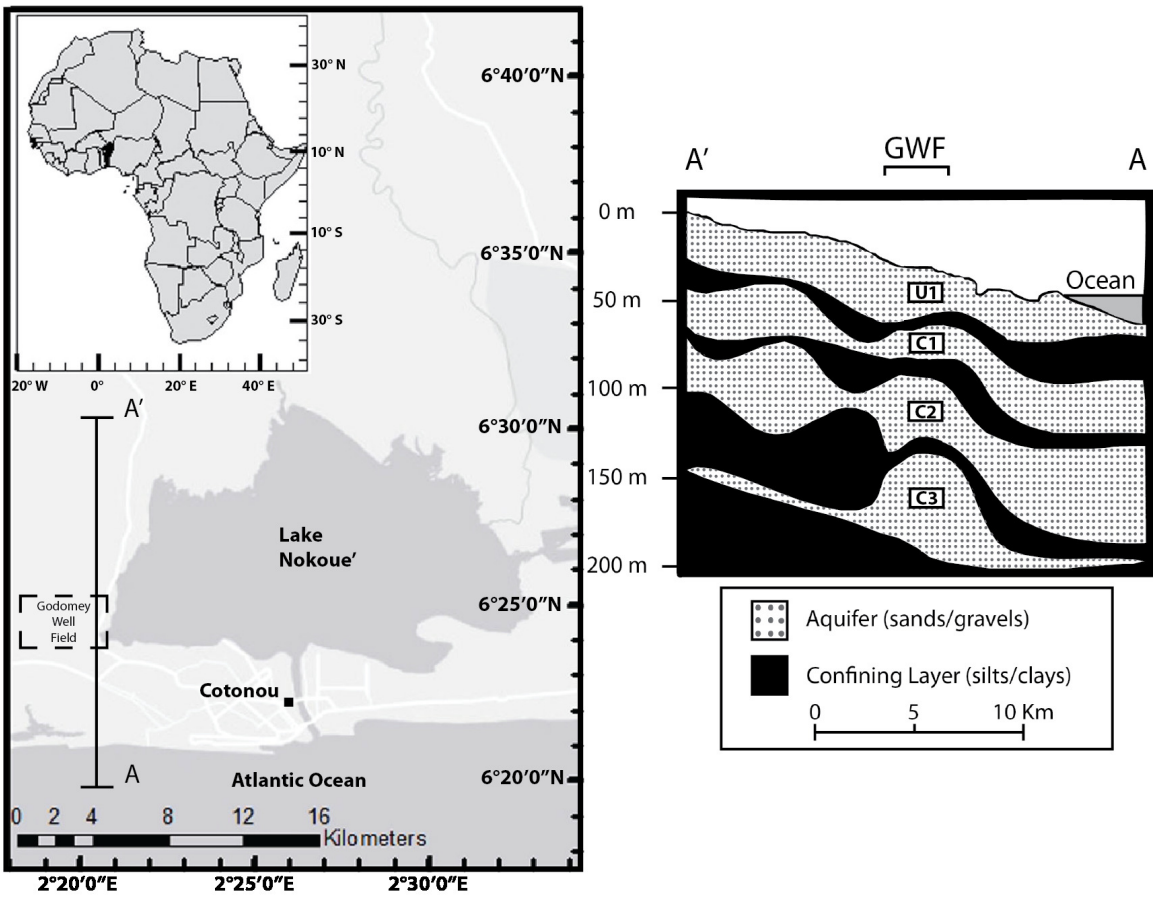


Figure 1.4: Schematic cross section of the regional geology along transect A-A'. GWF represents the location of the Godomey well field. The geology of the well field is comprised of an unconfined sand aquifer (U1) and three confined sand/gravel aquifers (C1, C2, C3). The confining layers are comprised of silts and clays (cross section modified from Silliman *et al.*, 2010).

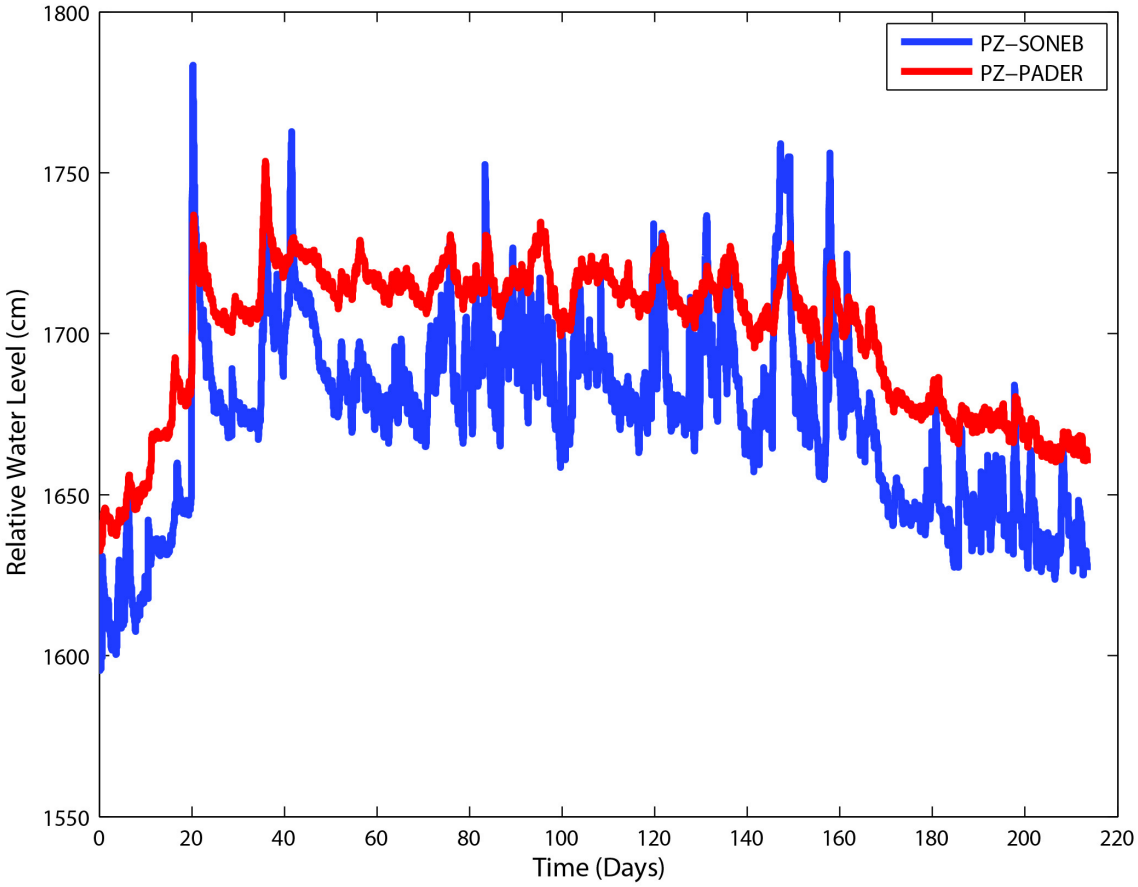


Figure 1.5: Relative water levels in piezometers PZ-SONEB (blue) and PZ-PADER (red) for a period of 210 days. The piezometers are located ∼1.3 km apart (Figure 2.3). PZ-SONEB is screened between 75-90 m depth and PZ-PADER is screened between 165-180 m depth. The aquifers between 75 - 90 m depth and 165 - 180 m depth are responding to variations in pumping pressure simultaneously, indicating aquifer confinement is not complete in this region, and the aquifers are hydraulically connected.Because the baseline for the water level is arbitrary, we added 400 cm to the PZ-SONEB data for easier comparison with the PZ-PADER data.

# CHAPTER 2

# GEOPHYSICAL SURVEYS

## 2.1 Summary

In this chapter I present the geophysical surveys I collected to characterize the Godomey aquifer. I would like to note that while I acquired multiple survey types, the majority of data collected did not help meet the study objectives due to many complicating factors, as will be discussed. The exception to this is the land seismic data that I collected, which will be the focus of Chapter 3. Even though certain surveys were unable to help meet study objectives, I believe it is useful to briefly discuss these surveys here, for the benefit of potential future work in the region.

## 2.2 DC Resistivity

A typical direct current (DC) resistivity survey injects either DC current or low frequency alternating current into the subsurface between two current electrodes. Two additional electrodes are then used to measure potential difference at different points on the surface. The ratio of the measured voltage to the input current is referred to as the resistance, which is related to the bulk resistivity of the subsurface.

Typically pore-water is by far the strongest contribution to subsurface resistivity measurements, making the DC resistivity method a commonly used technique for

groundwater exploration. When the ionic content of pore water is increased, due to chloride for example, resistivities drop significantly, making DC resistivity an ideal tool for saltwater intrusion problems. Many authors have shown the DC resistivity method to be highly effective at delineating the saltwater/freshwater interface in coastal regions affected by saltwater intrusion (Yang *et al.*, 1999; Batayneh, 2006; Sherif *et al.*, 2006; Adepelumi *et al.*, 2009; Nguyen *et al.*, 2009).

### 2.2.1 Acquisition

I collected a total of 10 surveys ranging in length from 100 m - 500 m. The surveys were located along the western edge of Lake Nokoué, along the same lines as the seismic surveys (refer to Figure 2.3). Acquisition parameters are given in Table 2.1. I inverted the apparent resistivity pseudo-sections for true resistivity using the RES2DINV software (Loke and Barker, 1995). An example of these results is shown in Figure 2.1.

One notable feature from these data is the low resistivity upwelling located between 80 m - 130 m (Figure 2.1). A local, hand-dug well for domestic use is located on top of this feature. The very low resistivity values (<10 ohm-m) are typical of saline water. The water in the well was identified as saltwater via communication with the well owner. This suggests that saltwater recharge is happening on a localized scale in the upper unconfined aquifer nearest the lake.

While these results are interesting, the DC resistivity data do not penetrate deep enough to provide any information regarding the deeper confined aquifers. This is due to two reasons. First, I was limited by my equipment. I only had access to the IRIS Syscal Kid resistivity meter, a system that is designed for rapid acquisition of shallow surveys, which is limited to 24 electrodes and a relatively low injection

| | |
|---|---|
| Recording instrument | IRIS, Syscal Kid Switch-24 |
| Electrode array | Wenner |
| Number of electrodes | 24 |
| Electrode spacing | 5 m |
| Injection Cycle | 4 s |
| Stack Max | 6 |
| Stack Min | 3 |
| Q max | 3 |

Table 2.1: Survey and recording parameters used for resistivity surveys.

current. The 5 m takeout cables gave a maximum current electrode spacing of 120 m for the Wenner array, limiting the depth of investigation to an approximate depth of 15 m by the AB/8 rule of thumb.

Second, the presence of very high conductivity clay layers and saline water limits the penetration depth of the current lines. Even with a larger system with more electrodes and greater injection current, I would require very large offsets to reach the target depth of 200 m, making this method unfeasible for this study.

## 2.3 Transient Electromagnetics

The transient electromagnetic (TEM) method is based on the principle of electromagnetic induction. In a typical TEM survey, sources and receivers are usually wire coils or loops, and in many surveys the source loop is also used as the receiver loop. The coils are described as either horizontal or vertical according to the plane in which the windings lie. An alternating electric current is run through the transmitter wire which induces a magnetic field, which in turn induces eddy currents in the subsurface. The current flow is then abruptly terminated and the receiver loop measures the rate of decay of the secondary field due to the induced eddy currents

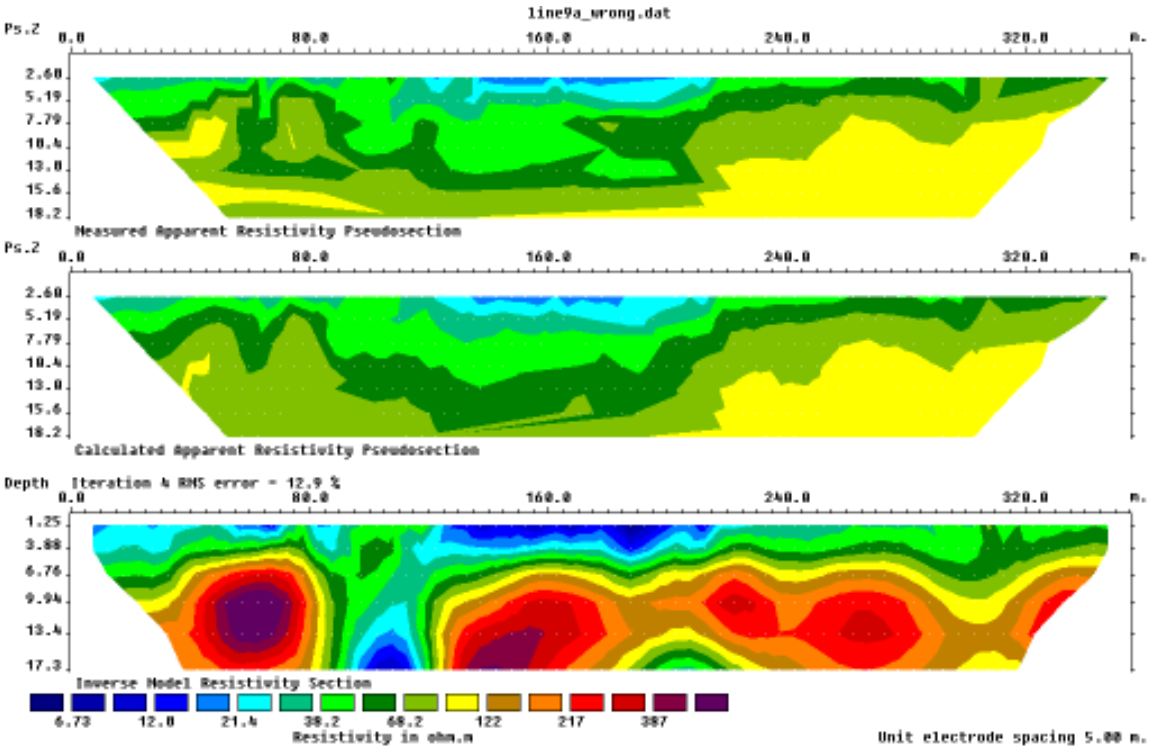


Figure 2.1: (top) Measured apparent resistivity for line 10a and (middle) calculated apparent resistivity for line 10a. (bottom) Inverted resistivity model for line 10a. The deepest penetration is approximately 17 m. The low resistivity upwelling between 80 m - 130 m is located near a domestic well that was confirmed by the owner to produce saline water.

in the subsurface. This decay curve can then help identify conductivity values of the subsurface through data inversion. The TEM method is frequently applied to a wide range of environmental problems, and is commonly used in groundwater exploration due to it's high sensitivity to conductive contaminants (e.g. saltwater) and clay layers that often represent impermeable boundaries to groundwater flow (Fitterman and Stewart, 1986; Metwaly *et al.*, 2001; Albouy *et al.*, 2001; Kontar and Ozorovich, 2006). Additionally, the TEM method provides significantly greater depth of penetration in

conductive environments relative to the DC resistivity method.

### 2.3.1 Acquisition

I collected a total of 12 TEM soundings, six were located along the western shores of Lake Nokoué and six were collected further inland and to the north of the well field. I used a Zonge GDP-16 NanoTEM system with a 30 x 30 m transmitter loop and 3 x 3 m receiver loop. I was extremely limited in the location of the measurements due to the presence of cultural noise in the survey area. All of the data from the TEM measurements were completely unusable, and is not included in this work. I believe that this was due to the cultural noise from the urban environment.

## 2.4 Seismic

The seismic reflection technique involves exciting a wavefield in the subsurface with a source and recording the resulting wavefield. While seismic reflection methods have been used in the oil and gas industry since the early 1900's, only in the last 35 years has the technique gained popularity for hydrogeological purposes (Steeples and Miller, 1990; Bachrach and Nur, 1998; Whiteley *et al.*, 1998; Cardimona *et al.*, 1998; Bradford, 2002; Bradford and Sawyer, 2002; Giustiniani *et al.*, 2008, 2009). In the coastal plain environment, fine grained material at the surface coupled with a shallow water table result in favorable conditions for seismic reflection surveys. While the seismic reflection technique cannot provide direct information regarding the distribution of saline water like the DC resistivity and TEM methods, it can provide greater depth of penetration, and may provide better vertical and horizontal resolution.

### 2.4.1 Marine Seismic Acquisition

I acquired marine seismic data within the western portion of Lake Nokoué encompassing the area from the Godomey well field south to the channel connecting the lake to the Atlantic Ocean. I used a novel source that is a mechanical adaptation of the pneumatic source developed by Pugin *et al.* (2003). Shot cycle time was approximately 1 s resulting in a shot spacing of about 3 m. The receiver was a single channel hydrophone recorded with a Geometrics 24-bit seismograph. Two example profiles of the data collected are shown in Figure 2.2.

Our seismic source generates a high frequency signal ($\sim$ 500 - 3000 Hz), providing very high resolution data in the upper 20 ms ($\sim$ 15 m), but no reflections are seen below this depth. Part of the reason for the lack of penetration is the presence of biogenic gas in the lake sediment (Figure 2.2 (bottom)). Biogenic gas rapidly attenuates high frequencies resulting in a lack of signal penetration (Bradford and Sawyer, 2002; Liberty *et al.*, 2009). The gas is present in the majority of the survey area and is most likely due to the decay of organic material (mostly palm stems) that has been brought into the lake by local fisherman to create fish habitats for fish farming. Gas is not present near the channel connecting the lake to the Atlantic Ocean (Figure 2.2 (top)). This region has not been manipulated for fish farming and is subject to tidal flushing, preventing the formation of gas zones. Due to the presence of gas and a high frequency source signal, the marine seismic data do not provide adequate depth of penetration in the capture zone near the well field and are not discussed further.

| | |
|---|---|
| Recording instrument | Geometrics, 24-bit, 120-channel seismograph |
| Receiver array | 10-Hz vertical geophones |
| Source | 10-kg sledge hammer |
| Geometry | in-line |
| Receiver spacing | 3 m (lines 1-11), 5 m (lines 12-13) |
| Source spacing | 6 m (lines 1-11), 5 m (lines 12-13) |
| Number of geophones | 48-120 |
| Sampling interval | 0.5 ms |
| Record length | 1 s |
| Record stacks | 5 (stacked in field) |

Table 2.2: Survey and recording parameters used for seismic surveys.

### 2.4.2 Land Acquisition

Land seismic data were collected along 15 transects during two field seasons for a total of approximately 9 km of reflection data (Figure 2.3) The study site is located in a large urban center which complicated data acquisition due to lack of road access and environmental noise caused by road traffic, construction and agricultural activities. Seismic profiles were chosen based on the above logistical considerations and research objectives. I focused the seismic acquisition on the eastern side of the Godomey well field to investigate the lateral continuity of hydrostratigraphic units between Lake Nokoué and the well field. I also collected data along two transects located near the center of the well field that are adjacent to three production wells.

Survey design parameters were chosen based on the primary objective of obtaining a high resolution image of the Godomey aquifer system (<250 m depth) and are given in Table 2.2. Despite the noisy cultural environment, surface conditions provided excellent source and receiver coupling resulting in data with a high signal-to-noise ratio as evidenced in Figure 2.4.

## 2.5 Discussion

The study site is located in a large urban center where logistical obstacles and high levels of cultural noise made many preferred survey sites either inaccessible or unfit for collecting high quality data. Addtionally, a lack of proper electrical resistivity equipment and the presence of biogenic gas in the lake sediment produced data that was insufficient for meeting project objectives. As stated previously, the electrical surveys and marine seismic surveys did not provide data that helped meet the project objective of refining the geometry of the Godomey aquifer hydrologic model. Despite this, the electrical resistivity and marine seismic surveys do provide high resolution data in the upper 15-20 m of the subsurface. While this data does not meet our project objectives, it may be of use for very shallow subsurface investigations in the area. These surveys also provide information about what kinds of sources and survey parameters may be necessary for deeper geophysical investigations in our study area. For example, future work in this area might include a marine seismic survey with a more powerful and lower frequency source that is able to image through the shallow gas zone in the lake (Liberty *et al.*, 2009). Additionally, future resistivity surveys targeting greater depths (>20 m) would benefit from using larger offsets, a greater injection current, and survey geometries targeted at deep investigation (pole-pole, pole-dipole).

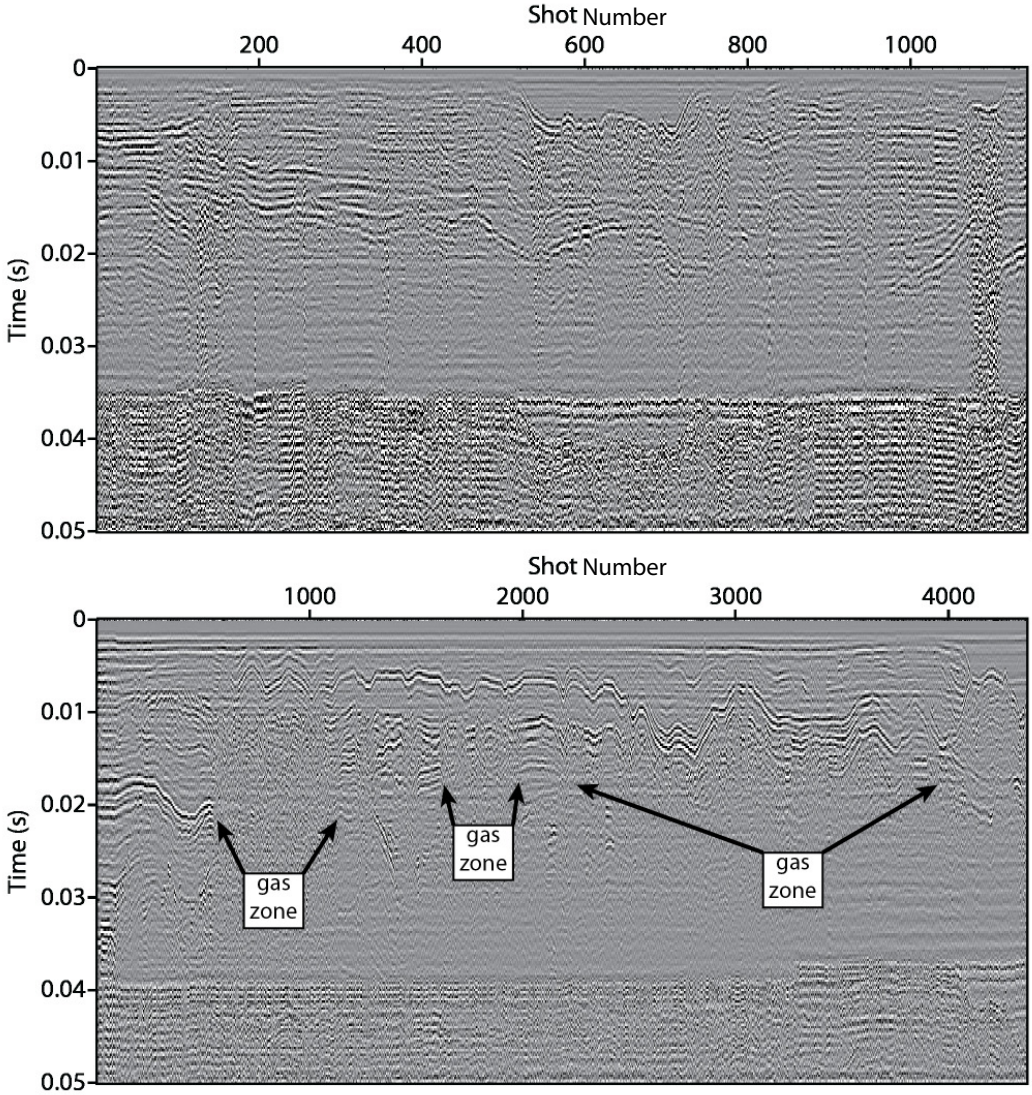


Figure 2.2: (top) Marine seismic section along a transect that crosses the channel connecting Lake Nokoué to the Atlantic Ocean. The center of the channel can be seen at shot number 600. This area has not been manipulated for fish farming and is subject to tidal flushing, preventing biogenic gas accumulation. (bottom) Marine seismic section along the western portion of Lake Nokoué in an area of intensive fish farming. Areas where biogenic gas is present have been identified by reflection hyperbolas generated by the gas pockets and 'shadow' zones beneath these gas pockets.

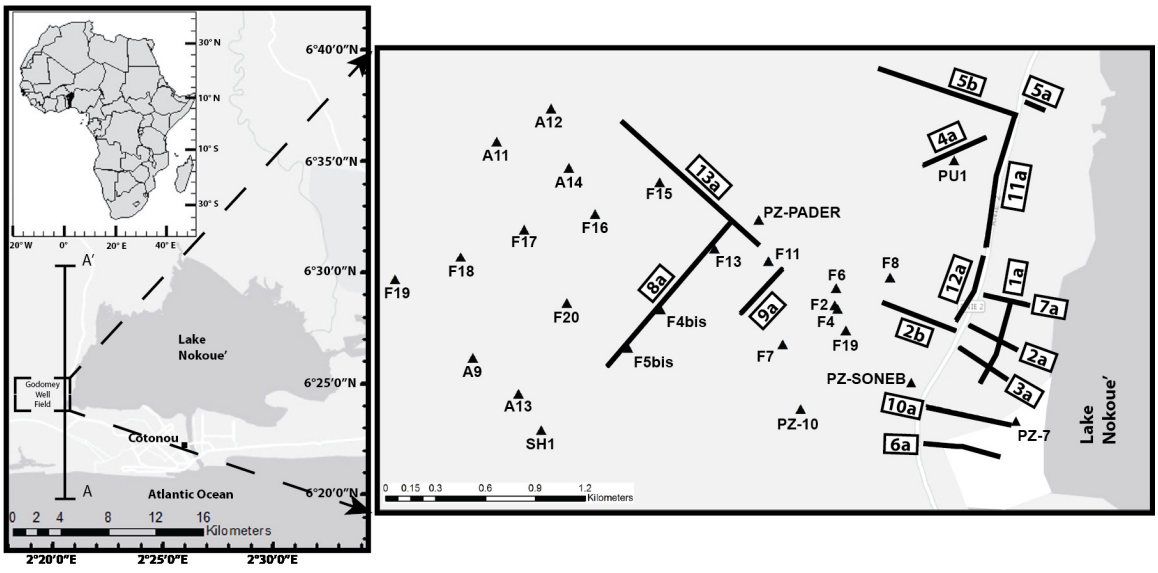


Figure 2.3: Map of the Godomey well field showing the locations of the 15 seismic profiles (black lines) acquired along with the location of wells and piezometers (triangles) in the area. Piezometers are labeled with the prefix PZ. All other triangles are production wells.

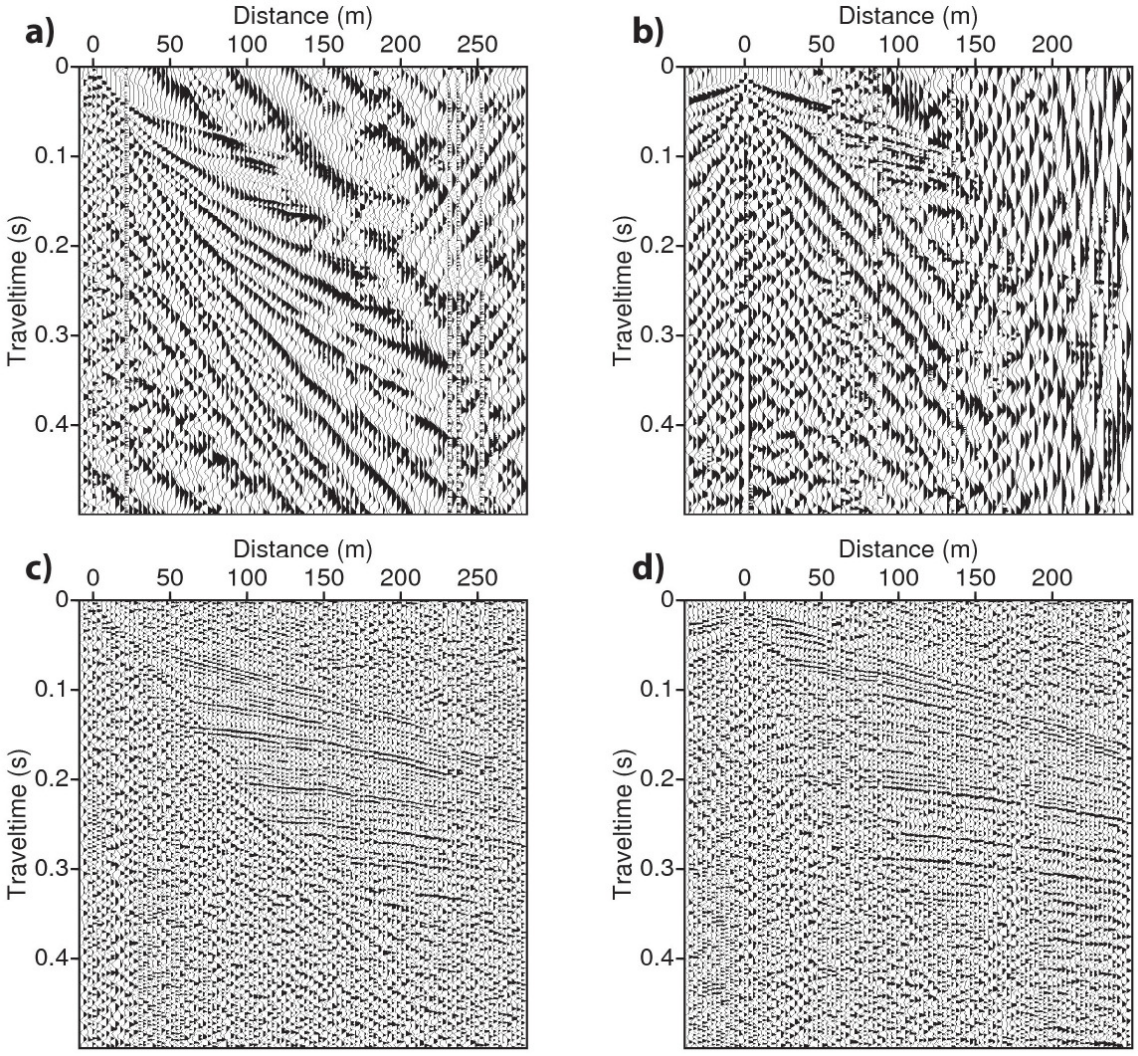


Figure 2.4: (a-b) Raw shot gathers from lines 5b and 6a respectively with AGC (50 ms window) applied for display. (c-d) The same shots with a spectral whitening filter (40-60-200-300 Hz) and AGC (50 ms window) applied to enhance reflections. Data quality is excellent despite the noisy urban environment, with clear reflections seen down to 400 ms. Note the effectiveness of the simple spectral whitening filter in removing high amplitude ground roll and traffic noise.

# CHAPTER 3

# DATA PROCESSING AND ANALYSIS

## 3.1 Summary

In this chapter, I present the processing flow and analysis of the land seismic data. Imaging and positioning problems are intrinsic to poststack migration methods due to the assumptions of normal moveout (NMO) processing, namely hyperbolic moveout and small lateral and vertical velocity variations. While the majority of the seismic transects I collected exhibit relatively flat lying reflectors and simple velocity fields that can be addressed with basic processing methods (Yilmaz, 2001), three of the transects contain stratigraphic complexity that likely violate assumptions of uniform stratigraphy. As a result, I apply two different processing strategies to the data.

I first discuss a routine processing flow using poststack time migration applied to the 12 transects with relatively flat lying reflectors. I then discuss the processing flow applied to the remaining three transects, which includes prestack depth migration (PSDM), residual moveout (RMO) analysis, and reflection tomography in the post migration domain. This approach improves velocity and image accuracy which helps to better constrain my interpretation (Guo and Fagin, 2002a,b; Bradford *et al.*, 2006, 2009a,b; Bradford, 2006, 2007; Bradford and Wu, 2007; Adler *et al.*, 2008). I do not include a discussion of the data processing for any of the other survey types collected (DC resistivity, TEM, marine seismic) as the surveys do not contribute to the project

goals and are therefore not relevant to the remainder of this work.

## 3.2 Seismic Data Processing

### 3.2.1 Simple Processing Flow

Processing steps applied to the 12 transects with little or no stratigraphic complexity (lines 1a, 2a, 2b, 3a, 4a, 5a, 6a, 7a, 9a, 11a, 12a, and 13a; refer to Figure 2.3.) were similar and shown in Figure 3.1. Pre-migration processing included spectral balancing (40-60-200-300 Hz) to enhance reflections and suppress ground roll, top muting to remove first arrivals, surgical muting to remove the noise cone, automatic gain control (AGC, window length = 50 ms) to boost amplitudes, elevation statics, stacking velocity analysis, normal moveout (NMO) corrections (stretch mute = 50%), residual statics to remove near surface irregularities, and common depth point (CDP) stacking. Figure 3.2 shows a CDP supergather (four adjacent CDPs summed) with various processing steps applied.

Because the data show some scattering of energy, I applied poststack time migration to the CDP stacked seismic profiles. I used a phase shift migration algorithm based on the method of Gazdag (1978) with a maximum migration frequency of 300 Hz and a maximum dip angle of 90 degrees. To derive the migration velocity models, I converted the smoothed stacking velocities to time-interval velocity models via a smoothed gradient method. The smoothed gradient method produces a smoothed time-interval velocity model using the Dix equation and cubic spline interpolation (see Dix, 1955).

Because of high levels of cultural noise, I did not attempt true amplitude processing and applied AGC early in my processing flow to enhance reflection signal. To

accurately compare depths between different seismic profiles, all profiles were moved to a final datum elevation of 43 m. This datum is the highest elevation of all 15 seismic transects and is located on line 8a near the center of the well field. The highest elevation was chosen for the datum due to the presence of a shallow water table. I completed all processing steps using ProMAX$^{TM}$.

### 3.2.2 Reflection Tomography Processing Flow

I applied a reflection tomography processing flow to lines 5b, 8a, and 10a (refer to Figure 2.3). The modeling flow adopted for this work is based on an iterative updating procedure for refining an initial depth-velocity model consisting of prestack depth migration (PSDM), residual moveout (RMO) analysis, and reflection tomography. RMO analysis is applied to common image gathers (CIG) that have been output from a prestack depth migration algorithm, and operates in the same way as conventional velocity analysis. If the migration velocity is incorrect, the reflection event is over-corrected or under-corrected, and the remaining moveout, or residual, is used as input to the reflection tomography to generate a corrected velocity model. At each iteration, both velocity and reflector geometries are updated until reflectors on CIGs are flay lying (Stork, 1992). A flow chart demonstrating the processing scheme is shown in Figure 3.1.

Pre-migration processing steps for lines 5b, 8a, and 10a were identical to the previous 12 lines up to velocity analysis (Figure 3.1). To derive a starting interval-velocity model in depth, I applied a dip moveout (DMO) correction prior to velocity analysis. I then converted the smoothed stacking velocities to depth-velocity models via the smoothed gradients method. I used a Kirchhoff migration method in the common offset domain and migrated the data from topography with a maximum frequency of

300 Hz and maximum migration aperture set to half the length of the spread. After two iterations of reflection tomography, there were no significant changes in velocity models and reflectors were sufficiently flat in the common image point domain. The PSDM images and final velocity models for lines 5b, 8a, and 10a are shown and discussed in Chapter 4.

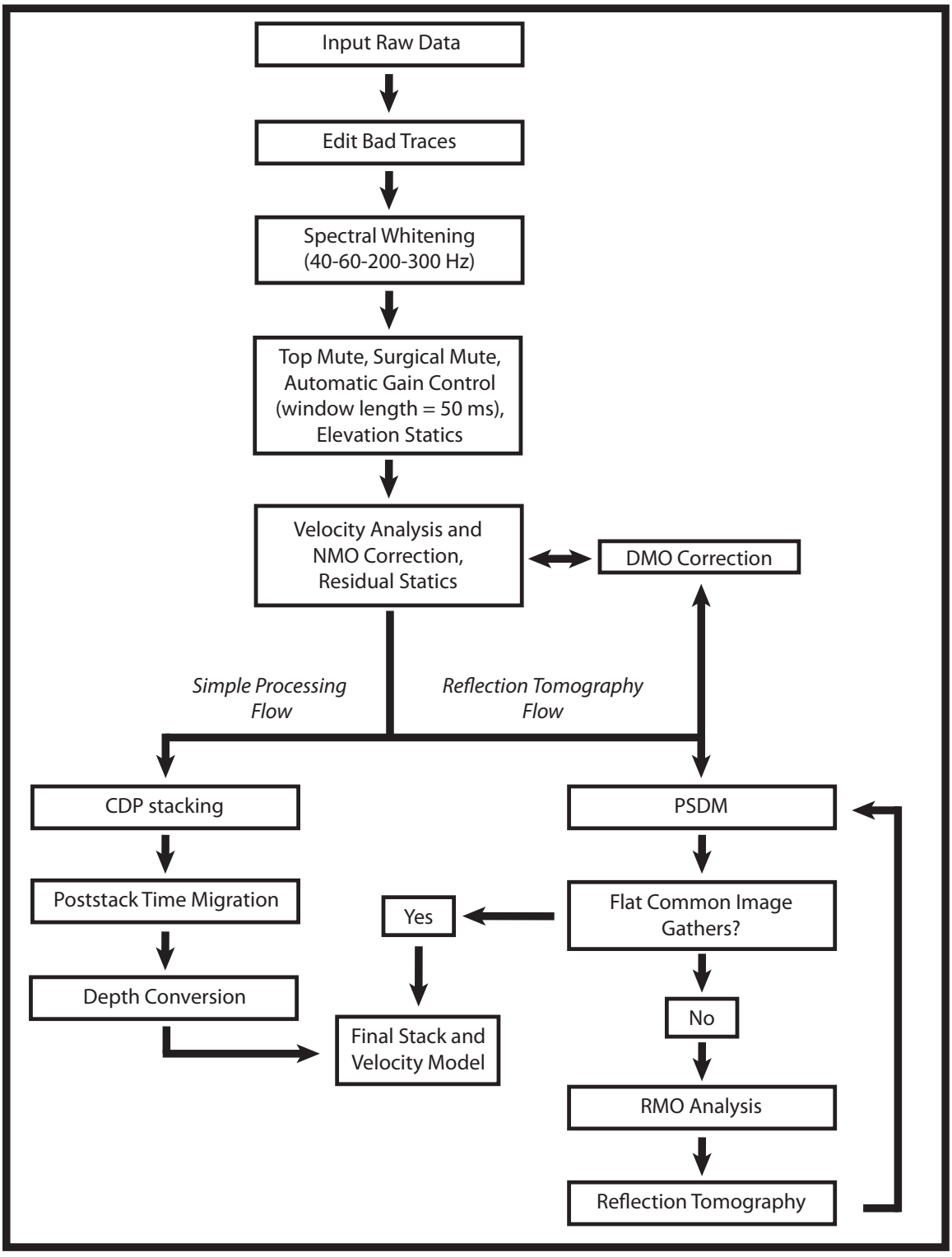


Figure 3.1: Flow chart illustrating the processing steps for both the simple processing flow (bottom left) and the reflection tomography flow (bottom right).

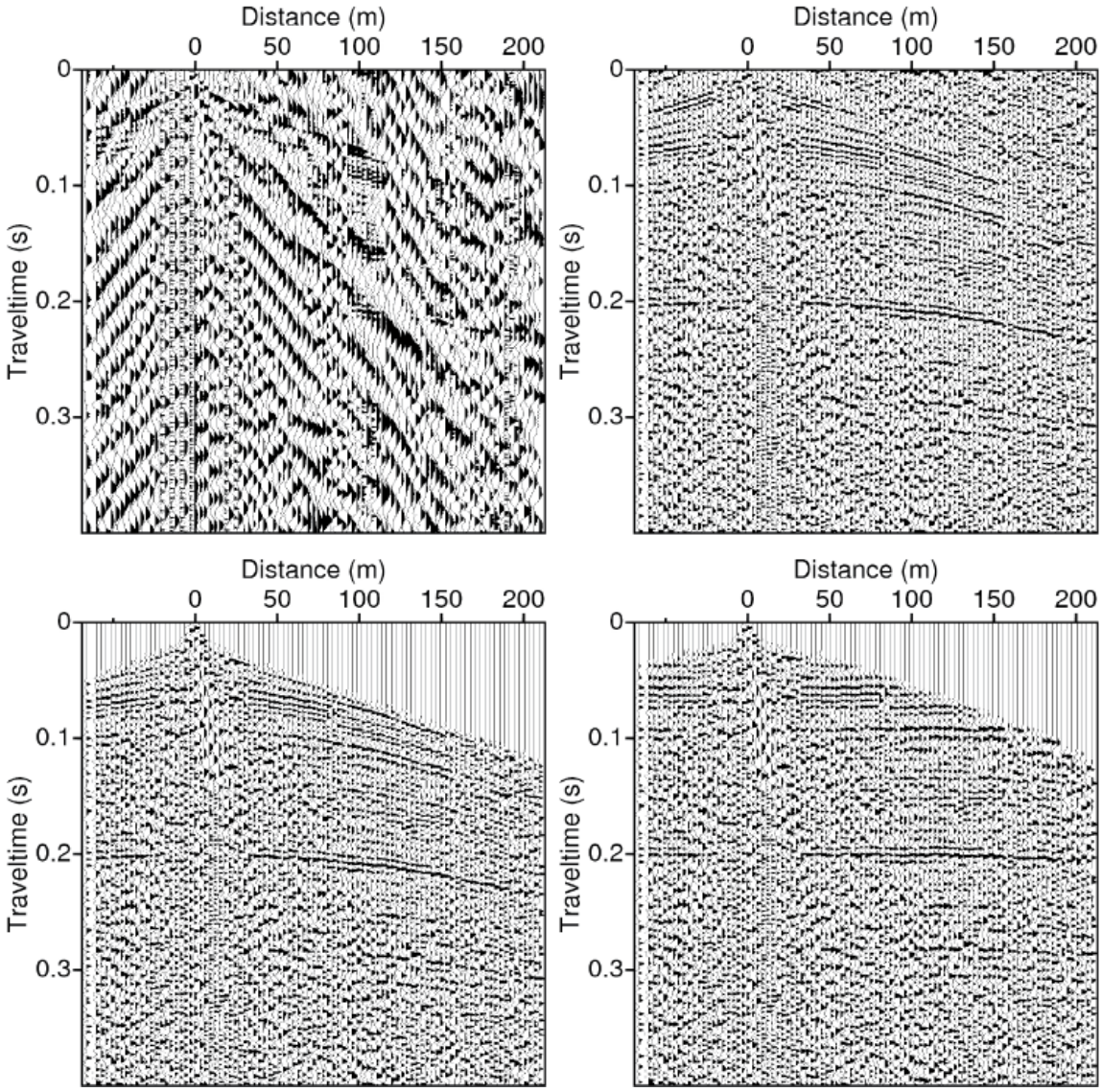


Figure 3.2: (top left) Raw CDP supergather (4 adjacent CDPs summed) from line 1a with (top right) spectral balancing (40-60-200-300 Hz), (bottom left) top mute, and (bottom right) NMO corrections. Note how flat the reflectors are after NMO correction.

# CHAPTER 4

# RESULTS AND INTERPRETATIONS

## 4.1 Summary

For geophysical surveys to be of any practical use, the data 'picture' needs to be represented as a geological cross-section. This conversion is done by utilizing prior geologic knowledge of the survey area, and/or, by actually estimating some physical properties of the subsurface from the measured data. In this chapter, I present the results of applying my processing strategy to the seismic data, and give my interpretations of the data based on the geology of the area.

## 4.2 PSDM Lines

I identified three distinct velocity zones from my tomographic inversion results that correlate with the top unconfined aquifer (U1), the three confined aquifers (C1, C2, and C3), and the clay/marl base (Figure 4.1). Based on the correlation with well logs from the area, I interpret the high amplitude reflections in the seismic data as the contacts between sand aquifers and confining clay layers (Figure 4.1d,f). A strong reflection at approximately 200 m depth is seen on all 15 profiles and is interpreted as the contact between aquifer C3 and the clay/marl aquifer base. This interpretation is based on the velocity increase from 1900 m/s to 2100 m/s (Figure 4.1b,d,f) and is

consistent with the expected depth of the clay/marl contact based on the geology of the area. For clarity, when I refer to depth, I refer to depth below the datum elevation of 43 m.

The dominant frequency of the reflections is about 80 Hz. Taking the average velocity to be about 1800 m/s gives a dominant wavelength of 22.5 m, giving a vertical resolution of approximately 5.5 m by the 1/4 wavelength rule (Widess, 1973). Using the 1/2 wavelength rule gives a more conservative, and probably more realistic, vertical resolution estimate of approximately 11.25 m. Given that the thicknesses of the confining clay layers range from 5 - 15 m, I do not expect to be able to fully resolve the confining clay layers with the seismic data.

### 4.2.1 Line 5b

Line 5b (Figure 4.1,a-b) shows most clearly the general hydrostratigraphy of the study area with the four primary aquifer units easily distinguished by the laterally continuous reflections. I interpret two channel features within the upper two aquifer units that extend from 50 - 300 m distance and 400 - 800 m distance (yellow dashed lines Figure 4.1b). This interpretation is based on the reflector geometry and low velocity zones located in the axes of these channels. The two high amplitude reflections beneath each of the channels at approximately 75 m depth (red dashed lines Figure 4.1b) have similar geometries to the overlying channels and are interpreted as older channel deposits in a stacked paleochannel sequence.

### 4.2.2 Line 8a

Line 8a (Figure 4.1c-d) is located near the center of the Godomey well field and runs adjacent to production wells F13, F4bis and F5bis. Lithology logs from the three

wells are plotted on the seismic section for comparison.

The thickness and depth of the unconfined aquifer is highly variable along this transect. The thickness of the unconfined aquifer increases from about 25 m depth in the south to approximately 50 m depth in the north, evidenced by the package of reflections between 30 m - 75 m depth on the southern half of the profile pinching out to a single reflection at approximately 50 m depth on the northern half of the profile. This interpretation is further supported by the well logs and the lateral velocity decrease of approximately 300 m/s from south to north. This velocity decrease correlates with the transition from clay to sand in wells F5bis and F4bis respectively. This observation is the opposite of what is expected as saturated clay is typically slower than saturated sand.

Definitive identification of aquifers C1, C2 and C3 is not possible across the transect due to the lack of reflections on the northern half of the profile between 60 m and 200 m depth (yellow dashed circle Figure 4.1d). Most notably, the strong reflection at 125 m depth, identified as clay in wells F4bis and F5bis on the southern half of the profile, is truncated at 600 m distance along the line. I interpret this to mean that aquifers C1, C2, and C3 are connected in this region due to an absence of confining clay layers. Note the absence of confining clay layers would not be predicted by the well logs due to the lack of depth penetration by well F13 (Figure 4.1d). One important point to note is that I lack dense ray coverage in this area for my velocity inversion due to the absence of reflectors. Therefore, the velocity in the region is not well constrained. Despite this issue, I believe my interpretation to be valid given the high quality of data and the chances of extreme lateral velocity variations are unlikely in my study area.

### 4.2.3 Line 10a

Line 10a (Figure 4.1e-f) runs approximately parallel to the lake shore with piezometer PZ7 located on the eastern end of the line. The lithology log from PZ7 is approximately 200 m deep and is plotted on the seismic section for comparison. The package of reflections between 50 - 110 m depth is related to interbedded clays and clayey sands based on the well log data. This package of reflections is cut between 75 - 150 m depth on the western portion of the transect by what I interpret as an erosional channel (yellow dashed line Figure 4.1f). My interpretation is supported by the lateral velocity contrast between the interpreted channel and aquifers C1 and C2.

## 4.3 Poststack Lines

Figure 4.2 shows the final stacked and migrated section for line 1a as an example of the results of my simple processing flow. Note that all reflectors are approximately flat lying, and dip slightly to the south at an angle of approximately 1°- 2°. The reflection from the clay/marl base is seen at approximately 230 ms, and is laterally continuous across the length of the transect. The package of reflectors between 75 - 110 ms is also laterally continuous across the length of the transect, and is interpreted as interbedded sands and clays based on the lithology log from nearby piezometer PZ7 (refer to Figure 2.3 for location of PZ7 and Figure 4.1 for lithology log). Between these two laterally continuous reflectors, it becomes difficult to confidently trace reflections across the length of the profile. I interpret this as a lack in continuity of confining clay layers, meaning that aquifers C1, C2, and C3 could be hydraulically connected in this area.

This can be seen more clearly in Figure 4.3, which shows a fence plot of the 9 lines closest to Lake Nokoué. The lateral continuity of the confining clay layers is highly variable along the southern portion of the lake, between the interpreted clay/marl base at 200 m depth (∼225 ms) and the interpreted clay layer at 70 m depth (∼100 ms). The four aquifer units (U1, C1, C2, and C3) are easily identified along lines 5b and 11a. South of line 11a, the confining clay layers become less distinct, and the confined aquifers are difficult to confidently distinguish (black rectangle in Figure 4.3).

Additionally, the continuation of the channel feature on line 5b is seen on lines 11a and 12a (black circle in Figure 4.3). This interpretation is supported by the absence of the shallow reflections in the upper 100 ms on these two lines, which are seen on all lines south of line 12a. This would orient the axis of the channel slightly southeast-northwest, running from Lake Nokoué through the northern portion of the Godomey well field.

## 4.4 Discussion

The lines closest to the lake and line 8a show abrupt discontinuities in confining clay layers suggesting aquifers C1, C2, and C3 are connected in the southern portion of the lake shore as well as further inland. These findings could explain the hydrologic data (Figure 1.5) that indicate the confinement of aquifers in this region is not complete, and aquifers C1, C2, and C3 are hydraulically connected. Hydraulically connected aquifers could have a substantial impact on the aquifer's response to intense pumping from the Godomey well field.

Erosional channels are present on lines 10a, 5b, and 11a, near the lake shore. The channel on line 5b and 11a appears to be cutting through the shallow package of clays

and clayey sands. I interpret the channel to be filled with saturated sands based on velocity estimates and well logs. Paleochannels filled with high permeability material, such as unconsolidated sands, could provide preferential flow paths for saline water from Lake Nokoué to the Godomey well field.

## 4.5 Conclusions

Seismic reflection profiles from the Godomey well field show the subsurface lithology to be a complex system of discontinuous and topographically variable strata. The current hydrologic model is based on a series of continuous sand, silt, and clay layers with little variability along dip. The seismic data prove these models assumptions to be invalid. The confining layers in the aquifer system are not continuous but show lateral variability on the scale of hundreds of meters. Additionally, there appear to be multiple locations of connectivity between confined aquifers due to the presence of erosional channels. These channels could be acting as preferential flow paths for saltwater between Lake Nokoué and the Godomey well field. The seismic data extends critical information about lithology to the surrounding area. This information can be integrated into the current hydrologic model to better constrain the geometry of the Godomey aquifer and improve model accuracy.

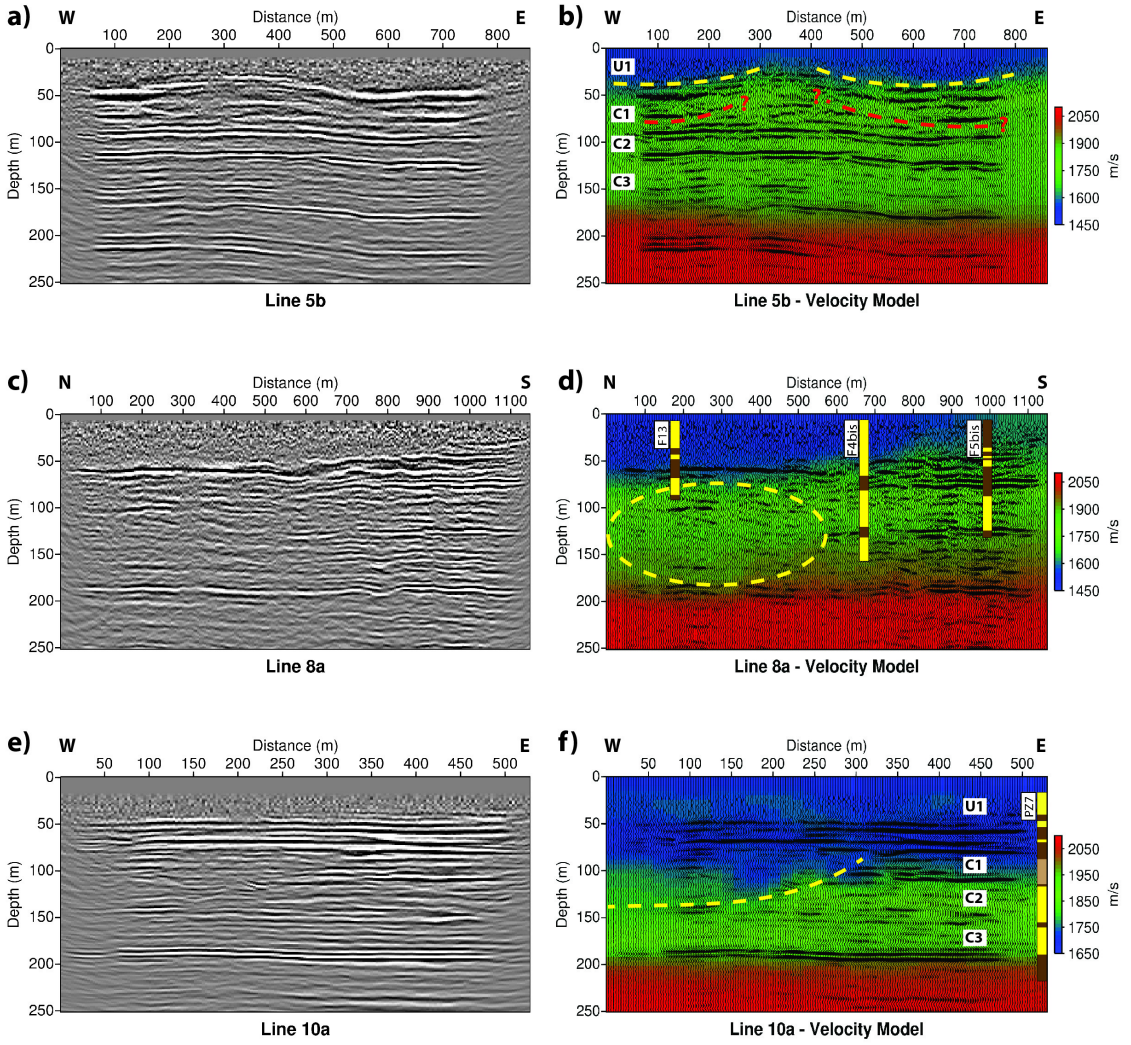


Figure 4.1: (a,c,e) PSDM sections for lines 5b, 8a, and 10a. (b,d,f) Interpreted PSDM sections overlain on final velocity models. Available well logs are overlain on lines 8a and 10a. Well log colors correspond to: yellow = sand, brown = clay, tan = clayey sand. U1 ranges in velocity from 1500 m/s to 1600 m/s on lines 5b and 8a. U1 has a higher velocity of 1700 m/s on line 10a, which is located next to Lake Nokoué. Velocities within the confined aquifers increase gradually with depth, starting at approximately 1700 m/s in C1 and increasing to 1900 m/s at the base of C3. The velocity jumps to 2100 m/s across the interpreted clay/marl base. Note the good correlation between clay layers identified in the well logs and high the amplitude reflections in the seismic data. Dashed lines indicate areas of interest discussed in the text.

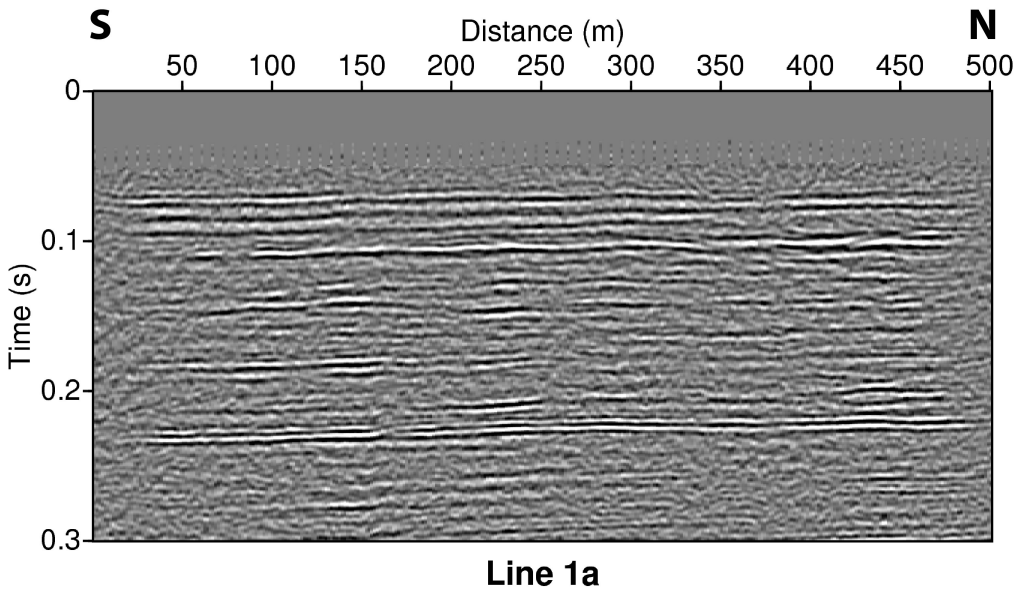


Figure 4.2: Poststack time migrated profile for line 1a. Reflectors at approximately 100 ms and the reflector at approximately 225 ms are laterally continuous across the entire transect, while reflectors between these two horizons are laterally variable with respect to their continuity. Note that all reflectors are flat lying with a slight dip (approximately 1°- 2°) to the south.

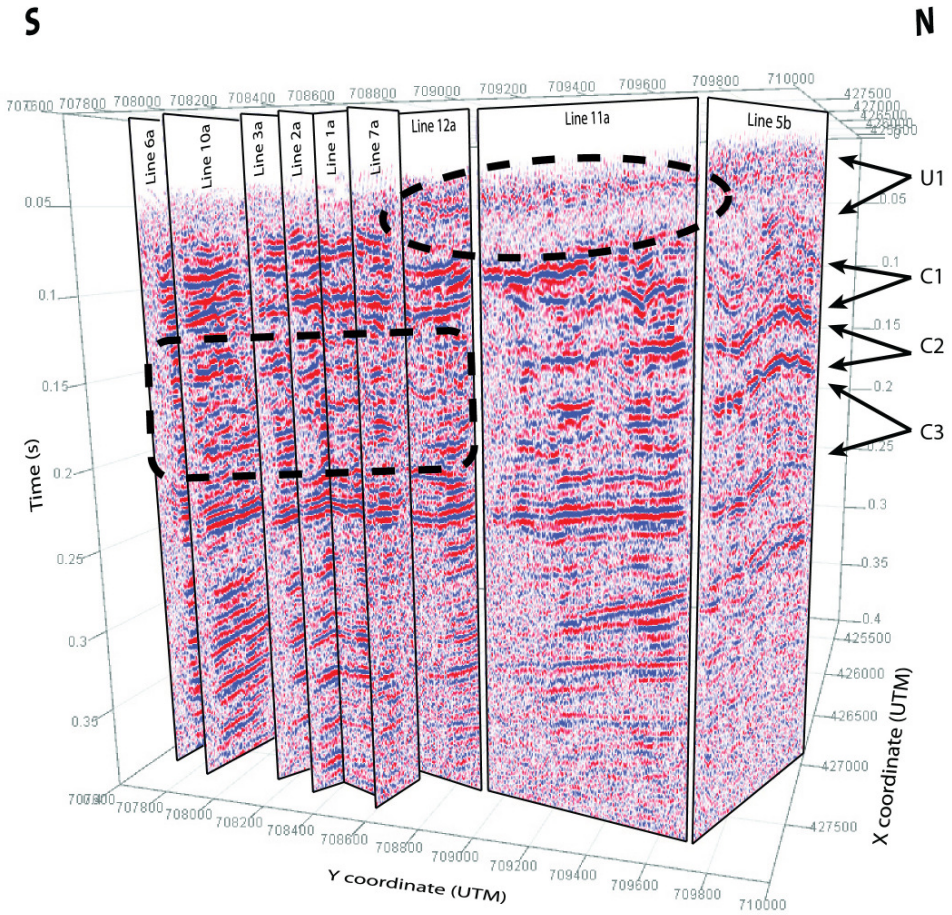


Figure 4.3: Fence plot of the time migrated sections of the 9 lines closest to Lake Nokoué. The view is looking to the southwest (refer to Figure 2.3). For comparison with the the poststack time migrated transects, the time migrated versions of lines 5b and 10a are shown. The labels U1, C1, C2, and C3 indicate the interpreted unconfined and three confined aquifers. The black dashed circle highlights the area of laterally discontinuous confining clay layers in the southern portion of the lake shore. The black dashed rectangle highlights the absence of shallow reflectors in the unconfined aquifer in the northern portion of the study area, which I interpret as the continuation of the channel feature on line 5b. Reflectors below the clay/marl base (>250 ms) dip to the south more steeply.

# CHAPTER 5

# HYDROLOGIC MODELING

## 5.1 Summary

In this chapter, I develop a hydrologic framework based on my seismic interpretations for use in a numerical hydrologic model of the study region. I review the existing hydrologic model developed by Boukari *et al.* (2008), and refine the model geometry in the region surrounding the Godomey well field based on my seismic reflection interpretations. In chapter 4 I discussed some of the small scale features (paleochannels and interconnected aquifers) identified in the seismic data. For the initial refinement of the hydrologic model, I do not incorporate these features and assume that all aquifers are completely confined, and refine the geometry of the original seven layer model (four aquifers and three confining layers) to best match the observed seismic data. While I recognize that this assumption simplifies the geometry of the aquifer and violates some of the observed seismic data, this initial refinement in modeling helps to identify how relatively local scale geophysical data can influence the predictions of a regional hydrologic model. Hence, this effort represents the initial step in a transition from a regional model based on sparse borehole data to a model with highly detailed local geology in the zone of production based on relatively dense seismic data. I find that under the same boundary conditions and pumping rates, the refined model predicts greater recharge from Lake Nokoué than the original model.

## 5.2 Introduction

A number of sequential studies have focused on developing a groundwater flow and transport model for the Godomey aquifer system (Boukari *et al.*, 2008; Borum, 2009; Silliman *et al.*, 2010). The most recent groundwater model has evolved from the initial steady-state model to a transient model that includes more complex distributions of hydraulic conductivity and density dependent effects (Borum, 2009). The initial effort by Boukari *et al.* (2008) modeled flow (without transport) assuming steady-state conditions for both the monthly mean well production data measured during the period from 1991 - 2000 and again for anticipated rate of production in 2011. This modeling resulted in two significant predictions regarding groundwater flow to the Godomey well field. First, that even under increased pumping rates a groundwater divide still exists between the Atlantic Ocean and the well field. Second, while low levels of recharge from Lake Nokoué were predicted based on the earlier study, significant recharge from Lake Nokoué was predicted under the 2011 pumping rates.

In order to best evaluate the impact of the seismic data on the prediction of hydraulic head, I refine the geometry of the initial steady-state state model. While I recognize that the most current model has been calibrated with more available data and includes transient behavior and density-dependent effects, I feel that refining the initial model without these complicating factors will provide the most direct estimate of the impact of modifying the aquifer geometry based on local scale seismic surveys.

## 5.3 Numerical Model

### 5.3.1 Conceptual Model

My conceptual hydrologic model was constructed using the Groundwater Modeling Software (GMS) program. GMS is a graphical software package that allows construction of a conceptual hydrological model for input to the MODFLOW finite-difference groundwater program developed by the Unites States Geological Survey (USGS). The numerical hydrologic model is 26 km in the east-west direction by 31 km in the north-south direction (Figure 5.1). It extends 27 km to the north of the coastline to a boundary defined by the mean piezometric contour of 15 m above mean sea level (amsl), and 4 km south of the coastline to the mean bathymetric contour of -10 m. The model is bordered on the east by the western portion of Lake Nokoué and the Sô River, and bordered on the west by a topographic depression known as the Dati Valley (Figure 1.3). Under natural conditions, the direction of groundwater flow is SSW. As such, the model was rotated 15° clockwise so that flow lines are approximately parallel to the grid.

The geological layers were constructed based on interpolation of lithologic logs from exploratory boreholes, pumping wells and piezometers. The aquifer was modeled as a homogeneous, horizontally-isotropic ($K_x = K_y \neq K_z$), three-dimensional system with seven layers, four of which are aquifers and three are confining layers (Boukari *et al.*, 2008). A variable grid size was used with the highest level of discretization being 230 m north-south x 250 m east-west around the well field, with cells gradually increasing with distance to a maximum dimension of 1850 m north-south x 1850 m east-west along the edges of the grid (Figure 5.1). The grid consists of 55 rows by 50 columns, for a total 2750 cells per layer.

### 5.3.2 Boundary Conditions and Parameters

To the north, cells in the first two layers that lie completely above the water table ('dry cells') were set as inactive. The northern most active cells in layers 3 - 5 were set to a constant head of 15 m amsl. To the south, cells in the first layer located within the Atlantic Ocean were set to a constant head of 0 m amsl. Cells in layer 1 located in Lake Nokoué, the Sô River, and the channel connecting Lake Nokoué to the Atlantic Ocean were set to a constant head of 0.5 m amsl. All cells in layers 2 - 7 located along the eastern, western and southern edges of the model were set as no-flow boundaries. The eastern part of the Djonou River is incorporated into the top layer using the river option in MODFLOW. The Bakamé and Dati valleys were modeled as drains using the drain option in MODFLOW. Layer 1 of the model was simulated as a free surface, allowing the water table to fluctuate in response to recharge.

Mean precipitation varies spatially and was modeled as three distinct recharge zones with values of 25 mm/yr in the northern part of the model, 100 mm/yr for the intermediate part of the model, and 200 mm/yr for southern coastal part of the model (Boukari *et al.*, 2008). The means of the monthly yield for each production well during the period of 1991-2000 were used for the steady-state simulations. These values range from 500 - 1800 $m^3/d$.

Initial estimates of horizontal and vertical conductivities as well as storage coefficients were based on available pumping data. These estimates were then adjusted by a trial and error calibration process to achieve an acceptable match between observed and predicted hydraulic head. Table 5.1 lists the values for horizontal and vertical conductivities as well as storage coefficients used in the model. Further details

| Layer | Horizontal Conductivity (m/s) | Vertical Conductivity (m/s) | Specific Storage ($S_s$) | Specific Yield ($S_y$) |
|---|---|---|---|---|
| 1 (U1) | $10^{-5}$ | $10^{-6}$ | $10^{-5}$ | 0.1 |
| 2 (clay) | $10^{-7}$ | $10^{-7}$ | — | — |
| 3 (C1) | 2 x $10^{-4}$ | 2 x $10^{-5}$ | $10^{-6}$ | 0.15 |
| 4 (clay) | $10^{-6}$ | $10^{-7}$ | — | — |
| 5 (C2) | 2 x $10^{-4}$ | 2 x $10^{-5}$ | $10^{-6}$ | 0.15 |
| 6 (clay) | $10^{-6}$ | $10^{-7}$ | — | — |
| 7 (C3) | 2 x $10^{-4}$ | 2 x $10^{-5}$ | $10^{-6}$ | 0.15 |

Table 5.1: Hydraulic conductivities of the Godomey aquifer system as they are implemented in the numerical groundwater model.

regarding the model and calibration process can be found in Boukari *et al.* (2008).

## 5.4 Refinement with Seismic Data

The seismic reflection data cover an areal extent of approximately 3 km x 3 km within the Godomey well field that corresponds to approximately a 13 x 12 cell grid in the discretized hydrologic model (Figure 5.1). To build the updated hydrologic model, I picked eight horizons on the seismic data that I interpreted as the tops and bottoms of the four aquifer units and three confining clay layers (Figure 5.2). These horizons were then interpolated to a 3 km x 3 km grid, discretized at 10 m. As discussed previously in chapter 4, I am not able to confidently resolve the top and bottom of the confining clay layers in many parts of the seismic data. For these areas, I simply picked the top and bottom of the wavelet to represent the top and bottom of the clay layer, fully recognizing that this results in some error in surface elevation. For the purposes of this study, the error in elevations will be negligible and I feel this approach is justified.

To incorporate these elevations into the existing hydrologic model, each horizon

was interpolated to a 13 x 12 cell grid (230 m north-south x 250 m east-west) to maintain the same resolution as the original hydrologic model. I then replaced the existing elevations of the eight horizons within the 13 x 12 cell grid with the new horizon elevations based on the seismic data. I then applied a 4 x 4 2-dimensional mean smoothing filter to the whole grid to remove the sharp contacts between the existing grid and the refined grid within the Godomey well field. Figure 5.3 shows an example of this procedure.

Figure 5.4 shows a comparison of cross sections between the original model and the updated model. It is visually evident that the smoothing procedure has significantly smoothed details along the edges of the model where cell discretization is coarsest. I tested different smoother lengths and found that the results of the finite difference model near the well field were relatively insensitive to the geology along the model boundaries. Therefore, even though the smoothed model oversimplifies the geology along the outer cells, there is no significant impact on the modeled hydraulic head results in the area of interest.

Table 5.2 shows the percentage difference in volume between the original aquifer model and the updated aquifer model within the areal coverage of the seismic data (red box Figure 5.1). The new model has increased volume in aquifers U1 and C1 and decreased volume in aquifers C2 and C3. The greatest change of the four aquifers is in aquifer C2, which has a decrease in volume by 55%. It is worth noting that this aquifer is the most intensely pumped of the four aquifers, and is responsible for 81% of total water withdrawn from all four aquifers (Boukari *et al.*, 2008).

| Aquifer | Percentage Difference in Volume |
|---|---|
| U1 (layer 1) | + 21 % |
| C1 (layer 3) | + 45 % |
| C2 (layer 5) | - 55 % |
| C3 (layer 7) | - 25 % |

Table 5.2: Percentage difference in aquifer volumes between the original hydrologic model and the updated hydrologic model.

## 5.5 Results

Figure 5.5 shows the steady-state head contours for both the original model and the updated model for aquifers U1 and C2. The two models were run with the same boundary conditions, initial conditions, and pumping rates. There are two notable features observed on the head contours for the updated model. First, the updated model predicts the 2 m amsl head contour, marking the groundwater divide between the Atlantic Ocean and the well field, migrates further to the west in aquifer U1. Second, the cone of depression within the well field has migrated approximately 400 m to the east, extending further out into the western edge of Lake Nokoué.

To evaluate the impact these differences in head contours have on groundwater recharge to the Godomey well field, I used the MODPATH package to track water particles from the western portion of Lake Nokoué and the eastern portion of the Djonou River. All particles were started from the water table. The results of the particle tracking are shown in Figure 5.6 and Figure 5.7. The results show that the expanded cone of depression leads to significantly more groundwater recharge being derived from both Lake Nokoué and the Djonou River.

## 5.6 Discussion

Presently, I have not been able to validate my updated model with any existing hydrologic data, making it impossible to conclude that I have improved the predictive capabilities of the existing model. Therefore, this work represents a sensitivity analysis from which I can derive valuable information.

Most importantly, decreasing the percentage volume of aquifer C2 by 55%, expands the zone of recharge captured by the Godomey well field by approximately 400 m. This extends the cone of depression further into Lake Nokoué than the original model, resulting in a significant contribution to groundwater recharge directly from Lake Nokoué. Similar contributions to groundwater from Lake Nokoué were predicted by the original model, but, under the projected 2011 pumping rates that were approximately three times larger than the pumping rates used in the current simulation. These results indicate that the modified aquifer geometry can produce recharge contributions from the lake that are equivalent to recharge contributions produced by increasing the pumping rates by a factor of three. This would suggest that Lake Nokoué is a significant source of salinity even under historical pumping conditions. Additionally, the increased recharge from Lake Nokoué increases the threat of anthropogenic pollution from the lake city of Ganvié. Combine this result with projected increased pumping rates, and Lake Nokoué becomes a major, long-term threat of anthropogenic pollution and saltwater intrusion.

The expanded zone of recharge also causes the lagoon region south of the Godomey well field to become active, which again, is only seen in the original model under the projected 2011 increased pumping rates. The updated model predicts that the surface water in the lagoon region, which is brackish, will account for a greater contribution

of recharge to the well field. In particular, more recharge will be derived from the Djonou River to the south, which is brackish for most of the year (Figure 5.7), thus increasing the threat of salt-water intrusion from this source.

Additionally, the southern lagoon region of concern coincides with land that is highly desired for urban development and agricultural use, particularly along the Djonou River. The increased contribution from surface water to groundwater recharge in the lagoon area increases the threat of anthropogenic contamination in the deep confined aquifers, and ultimately in the water produced in the well field.

## 5.7 Conclusions

Seismic reflection data were used to refine the geometry of an existing hydrologic model for the Godomey well field. Though the model has not been validated with existing hydrologic data to evaluate it's accuracy, the model provides useful insight into how recharge behavior is affected by modifying the aquifer geometry. Under the same historical pumping conditions, the updated model predicted a substantial contribution to groundwater recharge from two sources that pose a threat of saltwater intrusion into the Godomey well field: Lake Nokoué and the coastal lagoon region. Additionally, surface water recharge from both sources increases the likelihood of anthropogenic contamination due to the presence of the lake city Ganvié in Lake Nokoué, and industrial development and agricultural activities in the southern lagoon region. While the original model predicts similar outcomes, these predictions are based on the projected 2011 pumping rates that are three times higher than pumping rates used in this study. These results indicate that aquifer geometry plays a substantial role in the recharge behavior of the Godomey aquifer, and combined with projected increased

pumping rates, may indicate the threat to this freshwater resource is more immediate than previous studies suggest. Thus, the seismic results provide a potentially critical parameter for the groundwater model.

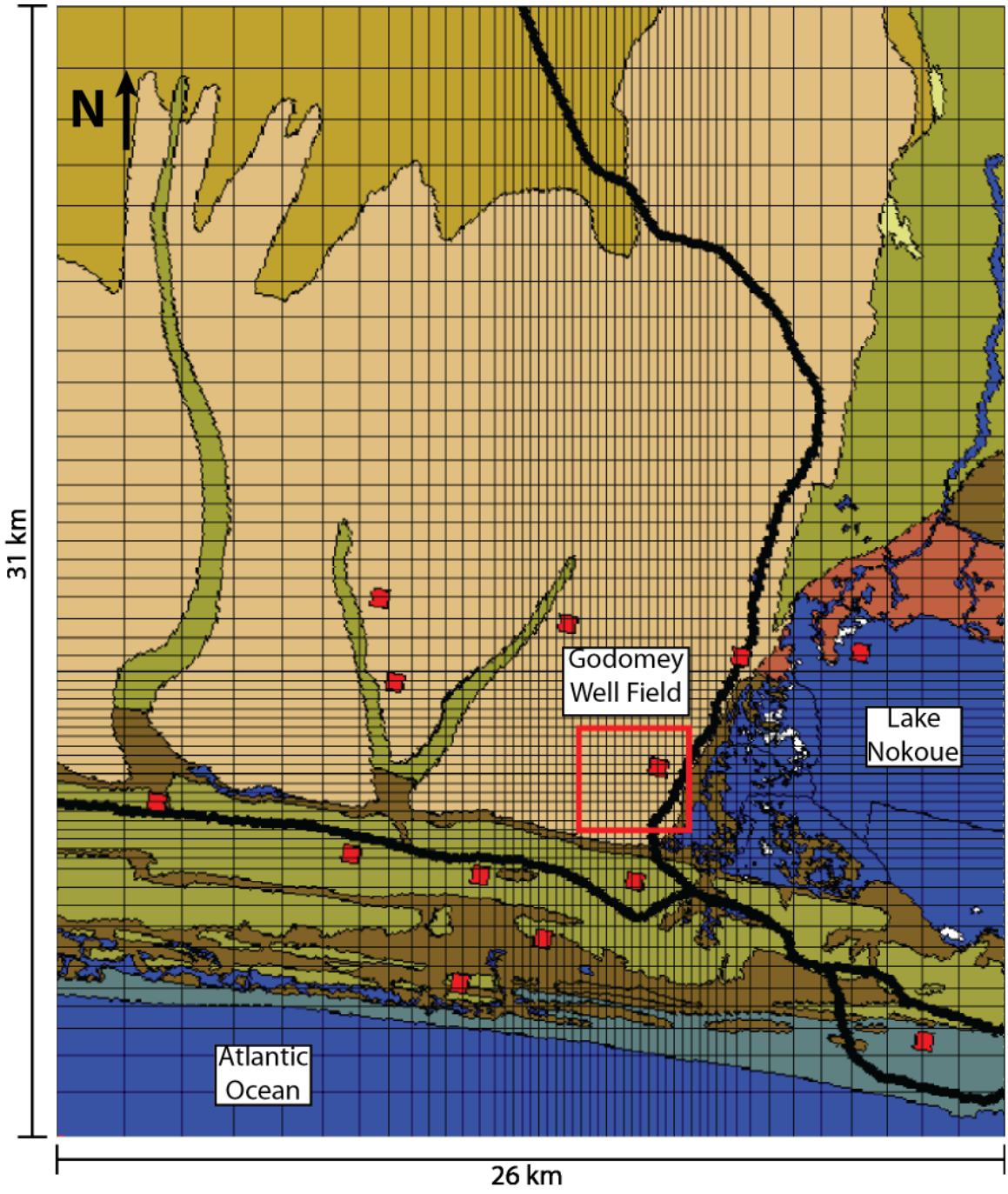


Figure 5.1: Map of the modeled area with finite-difference grid overlain. The red box shows the areal extent of the seismic data. The elevations of the cells within the red box were modified based on the seismic reflection data.

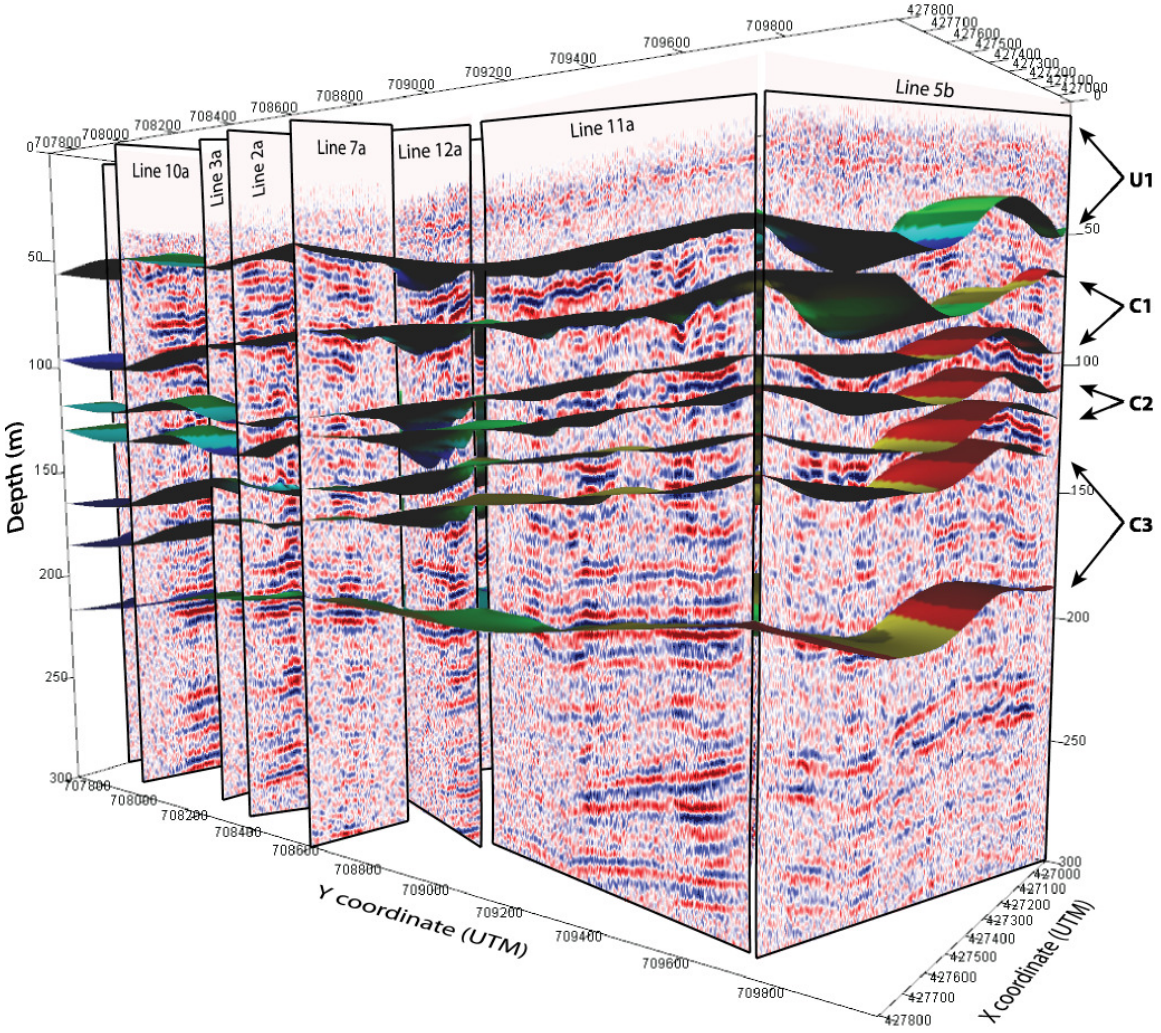


Figure 5.2: Fence plot of the depth converted time migrated sections of the nine lines closest to Lake Nokoué. The view is looking to the southwest (refer to Figure 2.3). The horizons delineate the tops and bottoms of the aquifer units and confining clay layers. U1, C1, C2, and C3 label my interpreted unconfined aquifer and three confined aquifers respectively. I have omitted the first horizon (surface elevations) for display purposes.

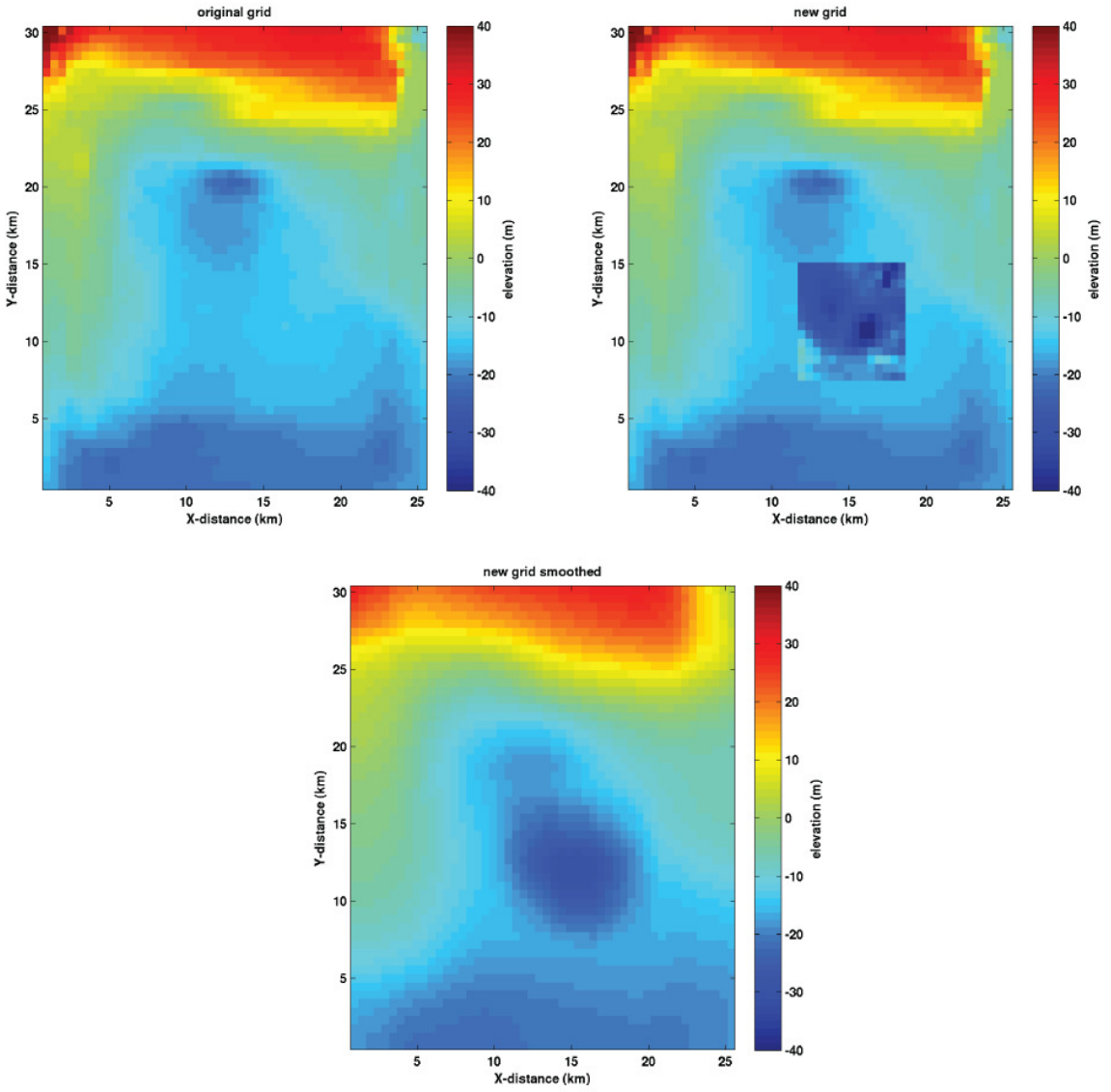


Figure 5.3: (top left) Original elevations for the base of the unconfined aquifer (second horizon). (top right) New elevation model with the updated grid around the Godomey well field based on the seismic data and (bottom center) the same elevation model after applying the two-dimensional smoothing filter.

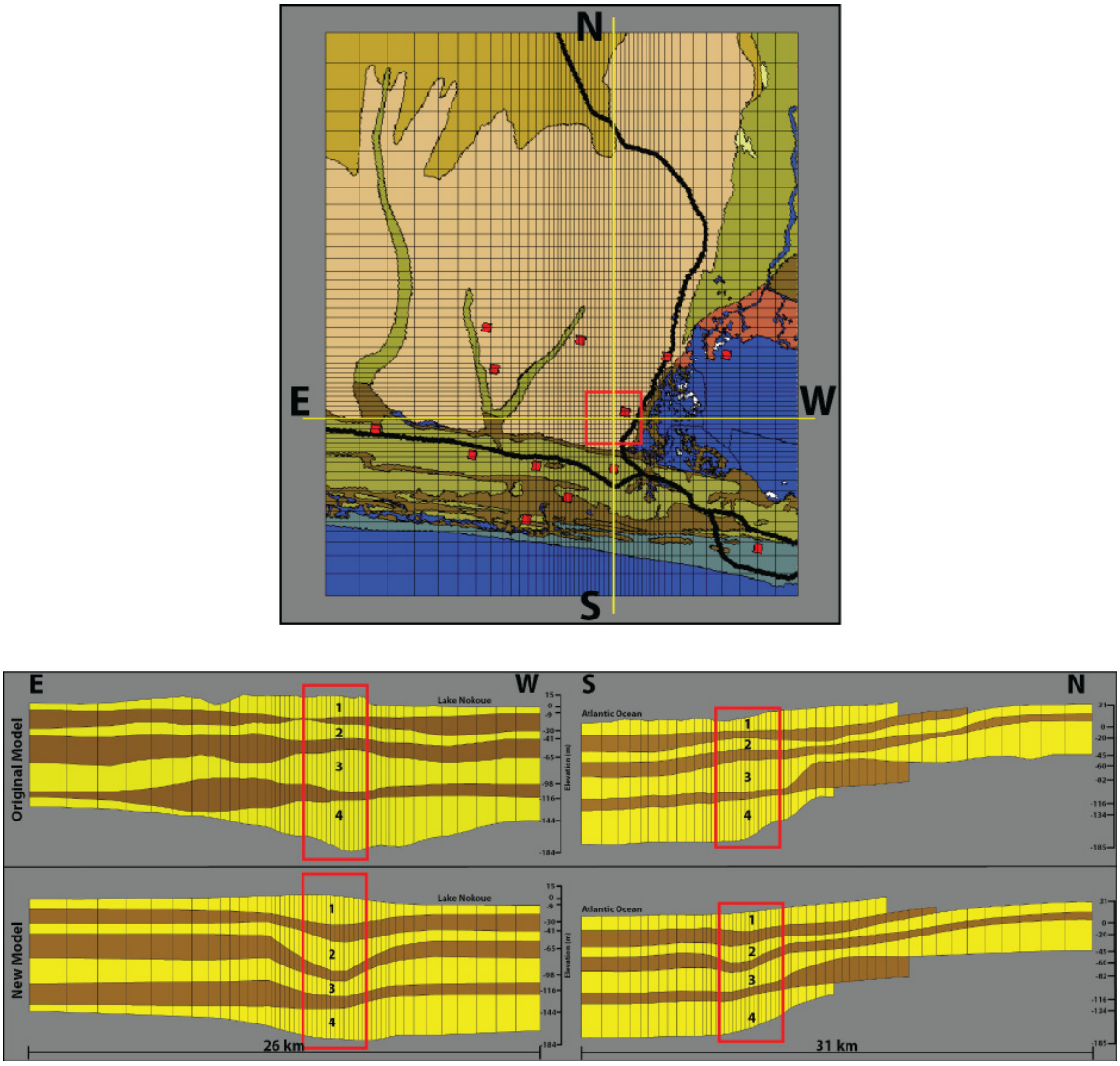


Figure 5.4: (top) Map showing the locations of cross sections E-W and N-S (yellow lines) that run through the center of the well field. (bottom) E-W and N-S cross sections comparing the original model (top) and updated model based on the seismic data (bottom). The red boxes indicates the portion of the grid that was modified. Aquifer layers are shown in yellow while the confining clay layers are shown in brown. The numbers identify the aquifers in order of increasing depth.

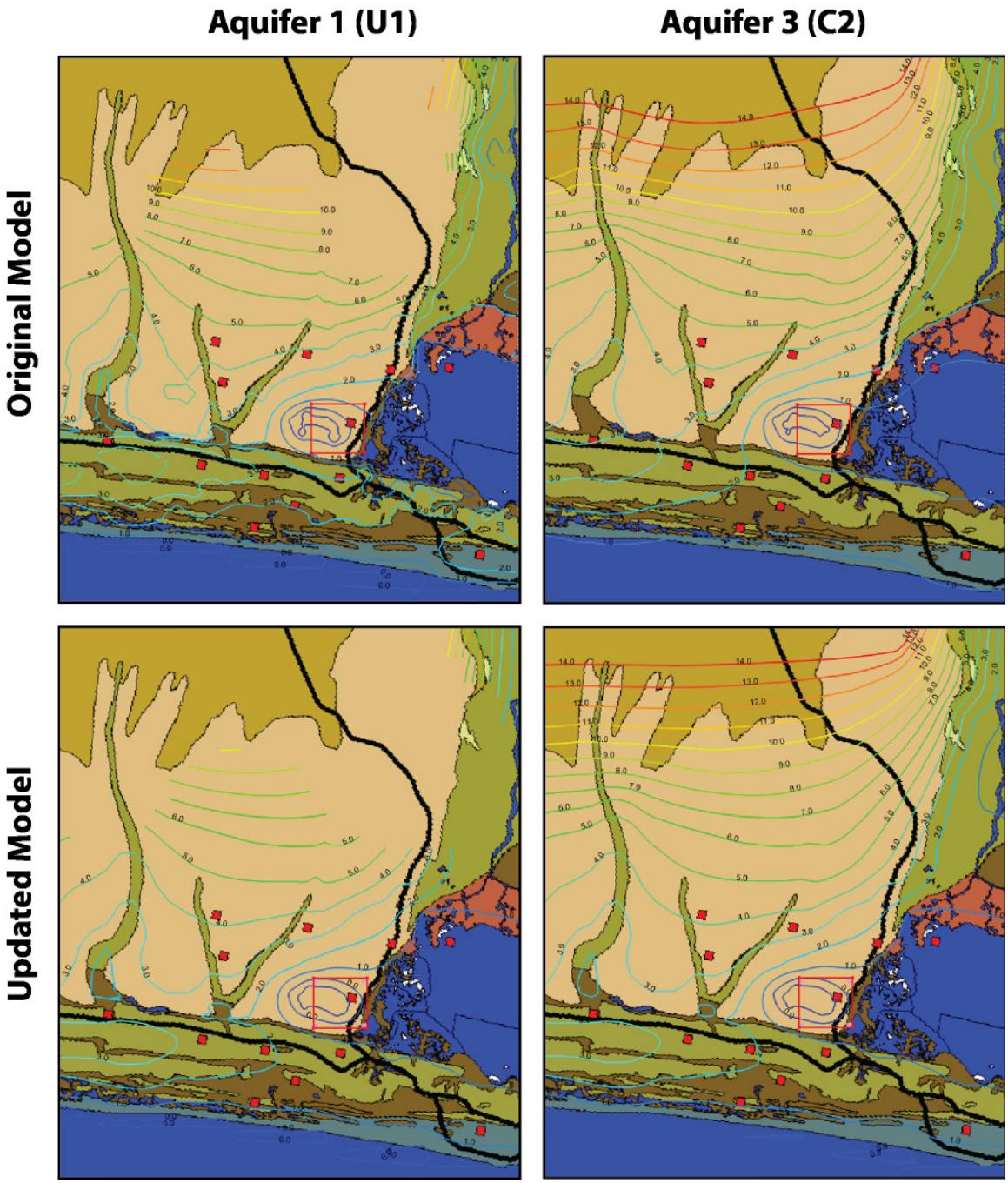


Figure 5.5: Map of predicted hydraulic head values for the original model in aquifer 1 (top left) and aquifer 3 (top right) compared with the map of predicted hydraulic head values for the updated model based on seismic data in aquifer 1 (bottom left) and aquifer 3 (bottom right). Warm and cool colored contour lines correspond to high and low hydraulic head values respectively. The areal extent of the seismic data is shown in the red box. The updated model predicts the cone of depression will expand by about 400 m within the region around the Godomey well field. The updated model also predicts the 2 m head contour, marking the groundwater divide between the Atlantic Ocean and the well field, has migrated to the west in aquifer U1.

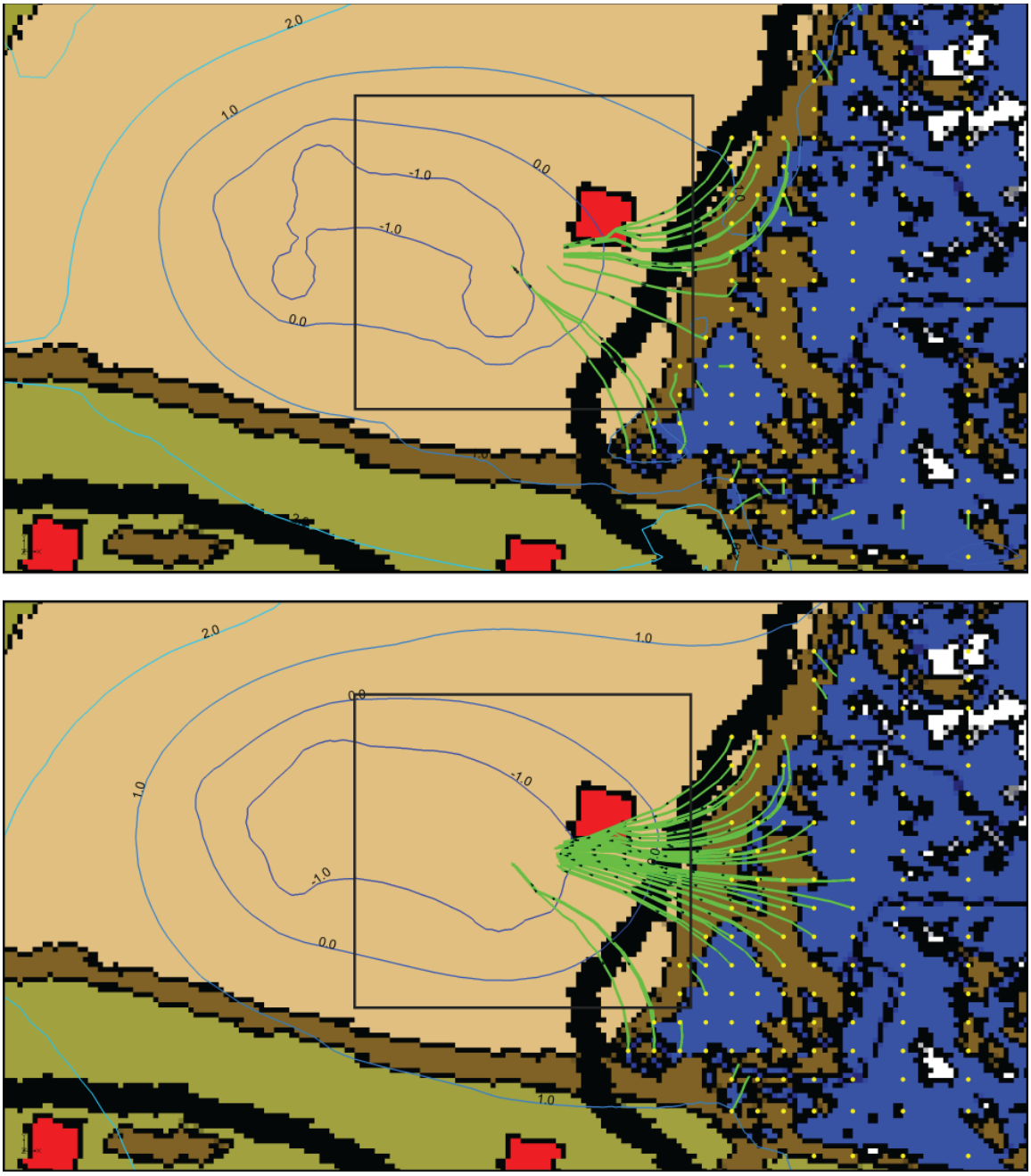


Figure 5.6: (top) Flow lines predicted by particle tracking for the original model and (bottom) the updated model based on seismic data. Particles were started at the yellow dots and the green lines indicated the path the particles take to the Godomey well field. The updated model predicts significantly more recharge from Lake Nokoué, making it a likely source of saltwater intrusion to the well field. The areal extent of the seismic data is show with black box.

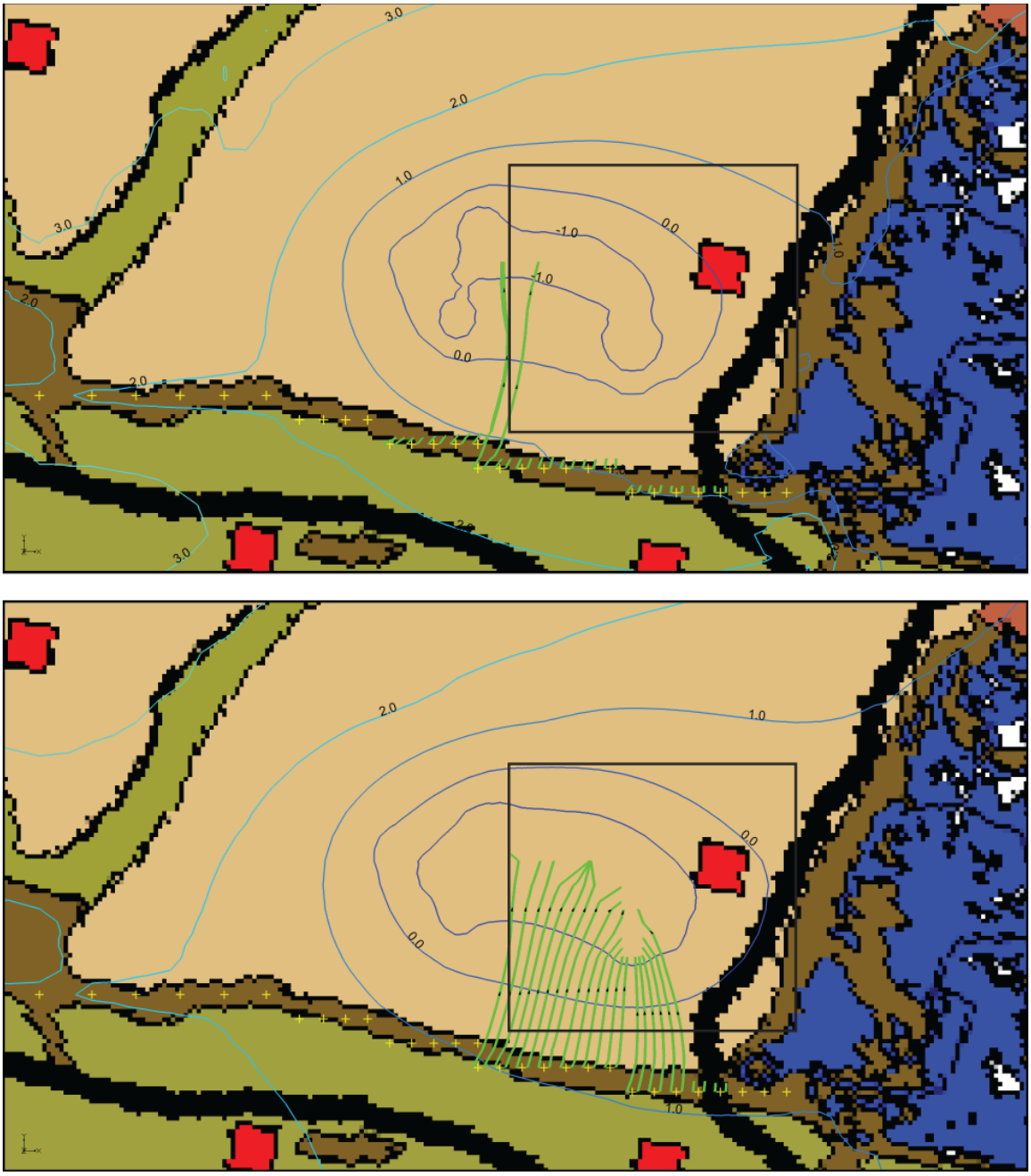


Figure 5.7: (top) Flow lines predicted by particle tracking for the original model and (bottom) the updated model based on seismic data. Particles were started at the yellow crosses and the green lines indicated the path the particles take to the Godomey well field. The updated model predicts significantly more recharge from Djonou River, making it a likely source of saltwater intrusion to the well field. The areal extent of the seismic data is show with black box.

# CHAPTER 6

# CONCLUSIONS AND DISCUSSION

## 6.1 Overview

The coastal city of Cotonou in Bénin, West Africa relies almost entirely on groundwater from the Godomey aquifer for its source of fresh water. The Godomey aquifer is currently threatened by the intrusion of saltwater into the primary production well field. To properly manage this problem, water agencies in Cotonou are in need of an accurate groundwater model to make reliable predictions of groundwater flow based on future management strategies. Initial efforts to build a regional aquifer model have had some success, but challenges still remain in terms of modeling the temporal and spatial distribution of hydraulic head. The current aquifer model is based on sparsely spaced borehole data. One of the key characterization needs identified to improve the model is mapping of the lateral continuity of the aquifer units and confining clay layers.

To address this problem, I collected a number of geophysical surveys to map the geometry of the Godomey aquifer. For this work, I focused primarily on land seismic surveys. In chapter 2 I discuss the survey design and acquisition parameters. Acquisition was focused on eastern portion of the Godomey well field in order to map the stratigraphy connecting the well field to Lake Nokoué, the likely source of the salinity. I collected 15 seismic transects for a total of approximately 9 km

of seismic data. Parameters were chosen to acquire a high resolution image of the Godomey aquifer system, which extends to a depth of approximately 200 m. I also discussed other geophysical surveys that I collected where the data quality was poor or depth of penetration was insufficient to contribute to this work. I have included that information for the benefit of potential future researchers.

In chapter 3 I discuss my processing strategy that I applied to the seismic data. While routine processing and poststack time migration were sufficient for the majority of the lines, three lines exhibited interesting complexity worthy of further investigation. For these lines I applied a processing flow that included PSDM, RMO analysis, and reflection tomography. This flow produced an accurate seismic image and velocity profile that helped constrain interpretation of these complexities.

Chapter 4 presented the results and interpretations of my processing strategy. I identified three distinct velocity zones from my tomographic inversion that correlate with the upper unconfined aquifer (U1), the three confined aquifers (C1, C2, and C3), and the clay/marl base. I also identified the presence of multiple erosional channels that provide connectivity between aquifer units. These channels could be filled with highly permeable sands and gravels, providing preferential flow paths between Lake Nokoué and the Godomey well field for saline water.

Finally, in chapter 5, I used the seismic reflection data to modify the geometry of the existing hydrologic model. This resulted in increasing the volumes of aquifers U1 and C1 by 20% and 45% respectively, and decreasing the volumes of aquifers C2 and C3 by 55% and 25% respectively. The resulting finite difference simulations predicted a significant increase in recharge from both Lake Nokoué and the coastal lagoon region, relative to the original model. These predictions are similar to predictions from the original model based on increased 2011 pumping rates, that are approximately

three times larger than the historical pumping conditions used for the updated model simulation. While I have not validated the updated model with hydrologic data, this result would mean that anthropogenic pollution and saltwater intrusion into the Godomey aquifer are more dire and immediate threats than previously suggested in prior studies.

## 6.2 Discussion

The seismic profiles in the vicinity of the existing well records enable us to correlate and extrapolate lithologies beyond the single data point at each well location. This information has been integrated into the current hydrologic model to better constrain the geometry of the Godomey aquifer and improve model accuracy. While previous studies have shown Lake Nokoué to be the primary source of salinity in the Godomey aquifer, the updated model suggests that saline water from Lake Nokoué may be recharging the Godomey aquifer more rapidly than previously thought, thus making the problem of salt water intrusion more immediate. Additionally, the updated model suggests that the Djonou River may also be a significant source of salinity to the Godomey well field, a threat that was not identified in previous studies. The implication of these findings is that any treatment or remediation plan must consider both the new threat of salt water intrusion from the Djonou River in the south and the immediacy of the threat to Cotonou's fresh water supply. The following are my thoughts on potential future geophysical surveys in the study region, the potential future of the hydrologic modeling, and recommendations on the current treatment strategy that has been proposed by the water agency in Bénin.

As stated previously, I have included a description of all geophysical surveys. Some

of these produced inadequate data for inclusion in this work. I have done this with the hopes that my successes and failures can be used as a guide for future geophysical work in the region, and I believe that there is still ample opportunity for geophysical investigations in Bénin and similar locations. In particular, there is still a severe lack of information about the geology underlying Lake Nokoué, which is a missing critical piece of information in the hydrologic model. Future work in this area might include a marine seismic survey with a more powerful and lower frequency source that is able to image through the shallow gas zone in the lake (Liberty *et al.*, 2009). Future research in this area would also benefit from deep electrical resistivity surveys in order to correlate stratigraphy from seismic reflection data with electrical conductivities. This would allow water agencies to target certain aquifers for pumping strategies based on electrical conductivity values (salinity). Resistivity surveys using larger offsets, a greater injection current, and survey geometry targeted at deep investigation (pole-pole, pole-dipole) could potentially reach the target depth of 200 m.

With regards to the hydrologic modeling, I believe that the work presented in this thesis is only the first step in building a completely refined hydrologic model. The obvious next step is to simulate the observed channels which are probably the most hydrologically significant outcome of the seismic study. The final step would be to incorporate the refined geometry into the most recent hydrologic model that has been calibrated with more data, and includes density-dependent effects that more accurately model groundwater flow in the presence of saltwater. This model then needs to be validated with transient models to compare predicted vs. observed hydraulic head, in order to evaluate whether the updated model improves prediction over the original model.

For this work, I retained the relatively coarse hydrologic model discretization in

order to avoid further refinement of the finite-difference grid. I believe future modeling efforts would benefit from finer discretization of the finite-difference grid in the area of the Godomey well field. This would allow the model to take full advantage of the high resolution seismic data, and also allow the incorporation of the local scale features, such as the erosional channels and interconnected aquifers, that are currently below the resolution of the finite-difference grid.

While the above considerations present many opportunities to improve the hydrologic model further, the intial model refinement presented in this work brings to light some recommendations for the initial treatment of salt water intrusion into the Godomey aquifer. The most significant of which would be to decrease the pumping pressure on aquifer C2. Aquifer C2 is currently the most intensely pumped aquifer with more than 80% of the well field yield coming from aquifer C2. The work presented in this thesis shows that the volume of aquifer C2 is 55% less than previously thought and likely the primary cause of the expanded cone of depression. Increasing pumping from aquifer C1, which this study has shown has a 45% greater volume than previously thought, and decreasing the pumping from aquifer C2, may slow the immediate advance of saline water from Lake Nokoué to the Godomey well field, while providing the same amount of total water yield.

Finally, due to the severity of the saltwater intrusion into the Godomey aquifer, water management agencies in Bénin are currently planning a new production well field about 8 km to the north of the Godomey aquifer. The present planning for this new well field does not include the acquisition of any geophysical data in the proposed new area of the well field. I believe this proposed project would benefit greatly from a seismic survey in terms of cost and effectiveness. Not only have countless case studies proven that drilling production wells informed by seismic reflection data increase

the chances of a productive well and decrease cost relative to drilling randomly, but the seismic data can be used for future modeling research similar to the work presented in this thesis. A proactive strategy like this is needed to properly manage this endangered resource in the face of climate change and population growth, in order to prevent this same scenario repeating itself.

# REFERENCES

Adepelumi, Adekunle Abraham, Ako, B.D., Ajayi, T.R., Afolabi, O., and Omotoso, E.J. 2009. Delineation of saltwater intrusion into the freshwater aquifer of Lekki Peninsula, Lagos, Nigeria. *Environmental Geology*, **56**(5), 927–933.

Adler, Frank, Baina, Reda, Soudani, Mohamed Amine, Cardon, Pierre, and Richard, Jean-Baptiste. 2008. Nonlinear 3D tomographic least-squares inversion of residual moveout in Kirchhoff prestack-depth-migration common-image gathers. *Geophysics*, **73**(5), VE13–VE23.

Alassane, A., Azonsi, F., and Boukari, M. 2009 (May). *Preliminary results of detailed inventory of transboundary aquifers in Benin, (West Africa).* Tech. rept. Department of Earth Sciences, University of Abomey-Calavi: Cotonou, Bénin.

Albouy, Yves, Andrieux, Pierre, Rakotondrasoa, Gérard, Ritz, Michel, Descloitres, Marc, Join, Jean-Lambert, and Rasolomanana, Eddy. 2001. Mapping Coastal Aquifers by Joint Inversion of DC and TEM Soundings-Three Case Histories. *Groundwater*, **39**(1), 87–97.

Bachrach, Ran, and Nur, Amos. 1998. High-resolution shallow-seismic experiments in sand, Part I: Water table, fluid flow, and saturation. *Geophysics*, **63**(4), 1225–1233.

Barthel, R., Jagelke, J., Götzinger, J., Gaiser, T., and Printz, Andreas. 2008. Aspects of choosing appropriate concepts for modelling groundwater resources in regional integrated water resources management–Examples from the Neckar (Germany) and

Ouémé catchment (Benin). *Physics and Chemistry of the Earth, Parts A/B/C*, **33**(1), 92–114.

Barthel, R., Sonneveld, B.G.J.S., Goetzinger, J., Keyzer, M.A., Pande, S., Printz, A., and Gaiser, T. 2009. Integrated assessment of groundwater resources in the Oueme basin, Benin, West Africa. *Physics and Chemistry of the Earth, Parts A/B/C*, **34**(4), 236–250.

Batayneh, Awni T. 2006. Use of electrical resistivity methods for detecting subsurface fresh and saline water and delineating their interfacial configuration: a case study of the eastern Dead Sea coastal aquifers, Jordan. *Hydrogeology Journal*, **14**(7), 1277–1283.

Blivi, Adoté, Anthony, Edward J., and Oyédé, Lucien M. 2002. Sand barrier development in the bight of Benin, West Africa. *Ocean & coastal management*, **45**(2), 185–200.

Borum, B.I. 2009 (August). *Draft Final Report: Mise au point professionnelle de la modélisation de la gestion des eaux souterraines du zone de Captage de Godomey, Cotonou, Bénin.* Tech. rept. Ministére des Affaires Étrangéres du Denmark: Copenhagen, Denmark.

Boukari, M., Gaye, C.B., Faye, A., and Faye, S. 1996. The impact of urban development on coastal aquifers near Cotonou, Benin. *Journal of African Earth Sciences*, **22**(4), 403–408.

Boukari, M., Viane, P., and Azonsi, F. 2008. Three-dimensional modeling of a coastal sedimentary basin of southern Benin (West Africa). *Applied Ground Water Studies in Africa, IAH selected papers on Hydrogeology*, **13**, 437–456.

Bowling, Jerry C., Harry, Dennis L., Rodriguez, Antonio B., and Zheng, Chunmiao. 2007. Integrated geophysical and geological investigation of a heterogeneous fluvial aquifer in Columbus Mississippi. *Journal of Applied Geophysics*, **62**(1), 58–73.

Bradford, John H. 2002. Depth characterization of shallow aquifers with seismic reflection, Part I-The failure of NMO velocity analysis and quantitative error prediction. *Geophysics*, **67**(1), 89–97.

Bradford, John H. 2006. Applying reflection tomography in the postmigration domain to multifold ground-penetrating radar data. *Geophysics*, **71**(1), K1–K8.

Bradford, John H. 2007. Frequency-dependent attenuation analysis of ground-penetrating radar data. *Geophysics*, **72**(3), J7–J16.

Bradford, John H., and Sawyer, D.S. 2002. Depth characterization of shallow aquifers with seismic reflection, Part II-Prestack depth migration and field examples. *Geophysics*, **67**(1), 98–109.

Bradford, John H., and Wu, Yafei. 2007. Instantaneous spectral analysis: Time-frequency mapping via wavelet matching with application to contaminated-site characterization by 3D GPR. *The Leading Edge*, **26**(8), 1018–1023.

Bradford, John H., Liberty, Lee M., Lyle, Mitch W., Clement, William P., and Hess, Scott. 2006. Imaging complex structure in shallow seismic-reflection data using prestack depth migration. *Geophysics*, **71**(6), B175–B181.

Bradford, John H., Nichols, Joshua, Mikesell, T. Dylan, and Harper, Joel T. 2009a. Continuous profiles of electromagnetic wave velocity and water content in glaciers: an example from Bench Glacier, Alaska, USA. *Annals of Glaciology*, **50**(51), 1–9.

Bradford, John H., Clement, William P., and Barrash, Warren. 2009b. Estimating porosity with ground-penetrating radar reflection tomography: A controlled 3-D experiment at the Boise Hydrogeophysical Research Site. *Water Resources Research*, **45**(4).

Bray, Ben, Tsai, Frank T.C., Sim, Youn, and Yeh, William W.G. 2007. Model development and calibration of a salt-water intrusion model in southern California. *Journal of the American Water Resources Association*, **43**(5), 1329–1343.

Cardimona, Steven J., Clement, William P., and Kadinsky-Cade, Katharine. 1998. Seismic reflection and ground-penetrating radar imaging of a shallow aquifer. *Geophysics*, **63**(4), 1310–1317.

Chen, Chao, Liu, Jiangping, Xia, Jianghai, and Li, Zhenyu. 2006. Integrated geophysical techniques in detecting hidden dangers in river embankments. *Journal of Environmental & Engineering Geophysics*, **11**(2), 83–94.

CIA. 2013. *The World Factbook*. https://www.cia.gov/library/publications/the-world-factbook/geos/bn.html.

Demanet, Donat, Renardy, François, Vanneste, Kris, Jongmans, Denis, Camelbeeck, Thierry, and Meghraoui, Mustapha. 2001. The use of geophysical prospecting for imaging active faults in the Roer Graben, Belgium. *Geophysics*, **66**(1), 78–89.

Dix, C. Hewitt. 1955. Seismic velocities from surface measurements. *Geophysics*, **20**(1), 68–86.

Ferguson, Ian J., Ristau, Johannes P., Maris, Virginia G., and Hosain, Ifti. 1999. Geophysical imaging of a kaolinite deposit at Sylvan, Manitoba, Canada. *Journal of applied geophysics*, **41**(1), 105–129.

Fitterman, David V., and Stewart, Mark T. 1986. Transient electromagnetic sounding for groundwater. *Geophysics*, **51**(4), 995–1005.

Gazdag, Jenö. 1978. Wave equation migration with the phase-shift method. *Geophysics*, **43**(7), 1342–1351.

Giustiniani, M., Accaino, F., Picotti, S., and Tinivella, U. 2008. Characterization of the shallow aquifers by high-resolution seismic data. *Geophysical Prospecting*, **56**(5), 655–666.

Giustiniani, Michela, Accaino, Flavio, Picotti, Stefano, and Tinivella, Umberta. 2009. 3D seismic data for shallow aquifers characterisation. *Journal of Applied Geophysics*, **68**(3), 394–403.

Guo, Ning, and Fagin, Stuart. 2002a. Becoming effective velocity-model builders and depth imagers part 1: The basics of prestack depth migration. *The Leading Edge*, **21**(12), 1205–1209.

Guo, Ning, and Fagin, Stuart. 2002b. Becoming effective velocity-model builders and depth imagers Part 2: The basics of velocity-model building, examples and discussions. *The Leading Edge*, **21**(12), 1210–1216.

Khalid, Malik. 2014 (July). *Human Development Report 2014*. Tech. rept. United Nations Development Programme.

Kontar, Evgeny A., and Ozorovich, Yuri R. 2006. Geo-electromagnetic survey of the fresh/salt water interface in the coastal southeastern Sicily. *Continental Shelf Research*, **26**(7), 843–851.

Lafia, S. 2005 (September). *Document de politique Nationale de l'Eau: la gouvernance de l'eau au service du développement du Bénin.* Tech. rept. Ministére des Mines de l'Energie et del'Hydraulique: Cotonou, Bénin.

Liberty, Lee M., Pratt, Thomas L., Lyle, Mitchell, and Madin, Ian P. 2009. Neotectonic analysis of Upper Klamath Lake, Oregon: New insights from seismic reflection data. *Geological Society of America Special Papers*, **447**, 71–82.

Loke, M.H., and Barker, R.D. 1995. Least-squares deconvolution of apparent resistivity pseudosections. *Geophysics*, **60**(6), 1682–1690.

Metwaly, Mohamed, Elawadi, Eslam, Moustafa, Sayed S. R., and Al-Arifi, Nasser. 2001. Combined Inversion of Electrical Resistivity and Transient Electromagnetic Soundings for Mapping Groundwater Contamination Plumes in Al Quwy'yia Area, Saudi Arabia. *Journal of Environmental and Engineering Geophysics*, **19**(1), 45–52.

Nguyen, Frédéric, Kemna, Andreas, Antonsson, Arni, Engesgaard, Peter, Kuras, Oliver, Ogilvy, Richard, Gisbert, Juan, Jorreto, Sara, and Pulido-Bosch, Antonio. 2009. Characterization of seawater intrusion using 2D electrical imaging. *Near Surface Geophysics*, **7**(5-6), 377–390.

Pugin, André J.M., Overney, Gilbert, Hunter, James A., and Pullan, Susan E. 2003. Walking over water: seismic reflection data acquisition using a hand hammer. *SAGEEP Proceedings, San Antonio, Tex.*

Schwab, Klaus, Sala-i Martin, Xavier, and Greenhill, Robert. 2010 (September). *The Global Competitiveness Report 2010-2011.* Tech. rept. World Economic Forum.

Sherif, M., El Mahmoudi, A., Garamoon, H., Kacimov, A., Akram, S., Ebraheem, A., and Shetty, A. 2006. Geoelectrical and hydrogeochemical studies for delineating seawater intrusion in the outlet of Wadi Ham, UAE. *Environmental geology*, **49**(4), 536–551.

Shtivelman, V., and Goldman, M. 2000. Integration of shallow reflection seismics and time domain electromagnetics for detailed study of the coastal aquifer in the Nitzanim area of Israel. *Journal of Applied Geophysics*, **44**(2), 197–215.

Silliman, Stephen E., Borum, Brian I., Boukari, Moussa, Yalo, Nicaise, Orou-Pete, Salifou, McInnis, Daniel, Fertenbaugh, Chrstyn, and Mullen, Andrew D. 2010. Issues of sustainability of coastal groundwater resources: Benin, West Africa. *Sustainability*, **2**(8), 2652–2675.

Silliman, Stephen E., Boukari, Moussa, Lougbegnon, Landry, and Azonsi, Felix. 2011. Overview of a multifaceted research program in Bénin, West Africa: An International Year of Planet Earth groundwater project. 175–186.

Steeples, Don W., and Miller, Richard D. 1990. Seismic reflection methods applied to engineering, environmental, and groundwater problems. *Geotechnical and environmental geophysics*, **1**, 1–30.

Stork, Christof. 1992. Reflection tomography in the postmigrated domain. *Geophysics*, **57**(5), 680–692.

Šumanovac, Franjo. 2006. Mapping of thin sandy aquifers by using high resolution reflection seismics and 2-D electrical tomography. *Journal of applied geophysics*, **58**(2), 144–157.

Vandenbohede, Alexander, Van Houtte, Emmanuel, and Lebbe, Luc. 2009. Sustainable groundwater extraction in coastal areas: a Belgian example. *Environmental geology*, **57**(4), 735–747.

Werner, Adrian D. 2010. A review of seawater intrusion and its management in Australia. *Hydrogeology journal*, **18**(1), 281–285.

Whiteley, R.J., Hunter, J.A., Pullan, S.E., and Nutalaya, P. 1998. Optimum offset seismic reflection mapping of shallow aquifers near Bangkok, Thailand. *Geophysics*, **63**(4), 1385–1394.

Widess, M.B. 1973. How thin is a thin bed? *Geophysics*, **38**(6), 1176–1180.

Yang, Chieh-Hou, Tong, Lun-Tao, and Huang, Ching-Feng. 1999. Combined application of dc and TEM to sea-water intrusion mapping. *Geophysics*, **64**(2), 417–425.

Yilmaz, Özdoğan. 2001. *Seismic data analysis*. Vol. 1. Society of Exploration Geophysicists Tulsa.